NASA Technical Memorandum 84376

USAAVRADCOM Technical Report TR-83-A-16

A Flight Investigation of Roll-Control Sensitivity, Damping, and Cross-Coupling in a Low-Altitude Lateral Maneuvering Task

L.D. Corliss and G. Dean Carico

December 1983

National Aeronautics and Space Administration

United States Army Aviation Research and Development Command

NASA Technical Memorandum 84376 USAAVRADCOM Technical Report TR-83-A-16

A Flight Investigation of Roll-Control Sensitivity, Damping, and Cross-Coupling in a Low-Altitude Lateral Maneuvering Task

L. D. Corliss,
G. Dean Carico, Aeromechanics Laboratory, Research and Technology Laboratories,
U. S. Army Aviation Research and Development Command,
Ames Research Center, Moffett Field, California

National Aeronautics and
Space Administration

Ames Research Center
Moffett Field, California 94035

United States Army
Aviation Research and
Development Command
St Louis, Missouri 63166

Page intentionally left blank

Page intentionally left blank

SYMBOLS

$a_{(\ )}$	washout roots, 1/sec
ADI	altitude direction indicator
ASD	auto spectral density
A_{ICB}	lateral cyclic control input, deg
A_{SS}	roll-series servo command, deg
$\dot{A}_{PS}$	roll-parallel servo command, deg/sec
B_{SS}	pitch-series servo command, deg
B_{ICB}	longitudinal cyclic control input, deg
B_e	spectral density resolution bandwidth, r/sec
$\dot{B}_{PS}$	pitch-parallel servo command, deg/sec
$B_{1/2}$	half power spectral bandwidth, r/sec
$B_{1/4}$	quarter power spectral bandwidth, r/sec
C	output matrix
C_1	UH-1H collective-main rotor gearing (1.43 deg/in.)
C_2	UH-1H pedal-tail rotor gearing (4.07 deg/in.)
CSS	control stick steering (V/STOLAND system mode)
C_{SS}	collective-series servo command, deg
$\dot{C}_{PS}$	collective-parallel servo command, deg/sec
D_{SS}	directional-series servo command, deg
$\dot{D}_{PS}$	directional-parallel servo command, deg/sec
E	least squares cost function matrix
F	system matrix
G	control matrix
h	altitude (above ground), ft
$\dot{h}$	altitude rate, ft/sec
$\ddot{h}$	altitude acceleration, ft/sec^2

H	feed-forward gain matrix
HSI	horizontal situation indicator
I_x	moment at inertia about x body axis, ft-lb-sec^2
I_z	moment at inertia about z body axis, ft-lb-sec^2
J	quadratic-performance-index cost function matrix
K	feedback gain matrix
K_B	UH-1H rotor stabilizer bar gain, deg/deg/sec
$K_{p_{(\ )}}$	roll-rate gain, deg/deg/sec
$K_{q_{(\ )}}$	pitch-rate gain, deg/deg/sec
$K_{r_{(\ )}}$	yaw-rate gain, deg/deg/sec
$K_{\dot{h}_{(\ )}}$	altitude-rate gain, deg/ft/sec
K_{δ_θ}	pitch sensitivity, deg/in.
K_{δ_ϕ}	roll sensitivity, deg/in.
K_{δ_c}	collective sensitivity, deg/in.
K_{δ_D}	yaw sensitivity, deg/in.
$K_{\psi_{(\ )}}$	heading gain, deg/deg
$K_{2_{(\ )}}$	parallel servo command gain, deg/sec/deg
K_5	parallel servo complementary filter gain, deg/sec/deg
L_p	roll damping due to roll rate, 1/sec
L_q	roll damping due to pitch rate, 1/sec
L_δ	roll-control sensitivity due to lateral control, rad/sec^2/in.
MAN	manual mode; basic UH-1H configuration, servos off
MAN*	manual mode flown through SCAS servos; stabilizer bar on
MFD	multifunction display
MLS	microwave landing system
M_p	pitch damping due to roll rate, 1/sec
M_q	pitch damping due to pitch rate, 1/sec

M_{δ}	pitch-control sensitivity due to longitudinal control, rad/sec^2/in.
NOE	nap-of-the-Earth
N_r	yaw damping due to yaw rate, 1/sec
n_d	number of records per specified estimation
PR	Cooper-Harper pilot rating
p	roll rate, deg/sec
p_{com}	roll-rate command, deg/sec
Q	output-vector weighting matrix
q	pitch rate, deg/sec
q_{com}	pitch-rate command, deg/sec
R	system-input weighting matrix
$R_{A.B}$	control configuration: A = amount of roll damping, B = amount of cross-coupling
r	yaw rate, deg/sec
s	Laplace operator, 1/sec
S	feed-forward weighting matrix
SBO	stabilizer bar off; effects cancelled through augmentation
SCAS	stability and control augmentation system
Tacan	tactical area navigation
U	control input
U_p	pilot control input
u	airspeed, ft/sec
v	lateral airspeed, ft/sec
w	vertical velocity, ft/sec
W	weight, lb
X	state vector
x	aircraft position (x-axis aligned with runway), ft
Y	output vector

y	aircraft position (y-axis), ft
δ_{COL}	collective stick, in.
δ_D	yaw pedal position, in.
δ_θ	pitch-cyclic stick position, in.
δ_ϕ	roll-cyclic stick position, in.
ζ	damping ratio, dimensionless
θ	pitch attitude, deg
θ_{COL}	collective pitch, deg
$\sigma_{( )}$	standard deviation of time-history ( )
τ	time-constant, sec
τ_B	stabilizer bar time-constant, sec
τ_p	roll rate feedback lag time-constant, sec
ϕ	roll attitude, deg
ψ	heading, deg
ω	natural frequency, rad/sec

Subscripts

A	roll-series servo input
B	pitch-series servo input
C	collective-series servo input
D	directional-series servo input
m	model system

A HELICOPTER FLIGHT INVESTIGATION OF ROLL-CONTROL SENSITIVITY, DAMPING, AND CROSS-COUPLING IN A LOW-ALTITUDE LATERAL MANEUVERING TASK

Lloyd D. Corliss and Dean Carico

AVRADCOM Research and Technology Laboratories

SUMMARY

A helicopter in-flight simulation was conducted to determine the effects of variations in roll damping, roll sensitivity, and pitch- and roll-rate cross-coupling on helicopter flying qualities in a low-altitude maneuver. The experiment utilized the Ames UH-1H helicopter in-flight simulator, which is equipped with the V/STOLAND avionics system. The response envelope of this vehicle allowed simulation of configurations with low-to-moderate damping and sensitivity. A visual, low-level slalom course was set up, consisting of constant-speed and constant-altitude S-turns around the 1000-ft markers of an 8000-ft runway. Results are shown in terms of Cooper-Harper pilot ratings, pilot commentary, and statistical and frequency analyses of the lateral characteristics. These results show good consistency with previous ground-simulator results and are compared with existing flying-qualities criteria, such as those set forth in MIL-F-83300 and MIL-H-8501A.

INTRODUCTION

Fundamental helicopter stability and control characteristics, such as control sensitivity, damping, and cross-coupling of pitch, roll, yaw, and collective responses, vary widely with type of rotor system. These characteristics are known to have a significant influence on flying qualities for various modes of helicopter operation; of particular interest are the effects of the pitch-roll coupling.

A need exists to determine the effect of these characteristics on flying qualities during the performance of such military tasks as nap-of-the-Earth (NOE) flight. The purpose of this experiment is to contribute to a data base from which the development of new criteria for helicopter flying qualities or the extension of existing criteria can be made.

To address this need, an in-flight simulation experiment was conducted specifically to determine the effects of control sensitivity, damping, and cross-coupling for low-altitude operations. This experiment had been preceded by stability and control analyses and by ground-based simulation investigations that explored the effect on NOE-flying qualities of different rotor system design features, such as hinge offset, hinge restraint, lock number, pitch-flap coupling (ref. 1), and the contribution of stabilization and command augmentation systems (SCAS) (ref. 2).

The experiment reported here was conducted on a UH-1H helicopter equipped with a versatile digital control, display, guidance, and navigation system (V/STOLAND). This system was used to alter the characteristics of the basic UH-1H so as to vary the flying-qualities parameters under consideration.

In previous ground-based simulations, a lateral task, a longitudinal task, and a combination task were evaluated. In the experiment reported here, only a lateral task was considered; it consisted of S-turns around markers spaced along a runway and was flown at a speed of 60 knots and an altitude of 100 ft. Within the limitations of the aircraft's control power and the capabilities of the V/STOLAND system, configurations were selected for evaluation that encompassed the low-to-moderate range of damping and sensitivity.

In this report, the configurations studied, the task, and the UH-1H V/STOLAND helicopter are described, and experimental results and data are discussed. Appendix A provides a more detailed description of the configuration setup procedures and appendix B describes the V/STOLAND flight controls system, and also outlines the method used to cancel the control effects of the UH-1H stabilizer bar.

DESCRIPTION OF EXPERIMENT

Experimental Matrix

In this experiment, the lateral handling qualities of a helicopter performing near-terrain maneuvers were evaluated. Variations in roll-rate damping (L_p), yaw rate damping (N_r), and roll-control sensitivity (L_δ) were studied at several levels of pitch- and roll-rate cross-coupling (M_p and L_q). A summary of the variables in this study is given below and a list of configurations is shown in table 1.

1. Roll-rate damping (L_p = -2 to -8 sec^{-1}) and roll-control sensitivity (L_δ = 0.41 to 1.1 $rad/sec^2/in.$).

2. Two levels of yaw damping (N_r = -1.2 and -3.5 sec^{-1}).

3. Three levels of pitch-roll cross-coupling as measured by the ratios of the derivatives L_q/L_p and M_p/M_q (0.0, 0.25, and 0.5).

The longitudinal characteristics were those of a basic UH-1H "stabilizer-bar-off" (SBO) configuration, except that the pitch damping was augmented to a level of M_q = -2 sec^{-1}. The 60-knot, level-flight estimates of the SBO configuration derivatives are those from reference 3 and shown in table 2. The configuration MAN shown in table 1 is the basic UH-1H manual mode with stabilizer-bar-on and the configuration MAN* is a fly-by-wire version of the manual mode. The relationship between many of the test configurations and several flying-qualities criteria boundaries is shown in figure 1.

A brief discussion of the existing flying criteria from specifications MIL-H-8501A, AGARD 577, and MIL-F-83300, as they relate to roll damping L_p and roll-control sensitivity L_δ, is given below.

MIL-H-8501A- Three boundaries are shown in figure 1 that are generally accepted as minimums for adequate handling qualities. The 20°/sec/in. line is a maximum boundary on control effectiveness and pertains to all speeds (sec. 3.3.15). The remaining two boundaries are vehicle-dependent boundaries which are functions of vehicle weight and inertia. The first of these is determined by the expression $3(W + 1000)^{1/3}$ (sec. 3.3.18), which is for a minimum angular displacement at the end of 0.5 sec for a 1-in. lateral cyclic input. For a weight of 8000 lb (e.g., for a UH-1H helicopter) this results in a line with slope 2.6°/sec/in. at high values of L_p which converges

to a minimum control sensitivity (L_δ) of 2.6°/sec^2/in. at zero L_p. This specification is based on a measurement made while in hover but is not restricted to a particular speed range; it is shown in figure 1 as the left-most 8501A boundary. The third boundary is a minimum roll damping for all weather operations and is also a hover-based measurement without any speed-range restrictions. This minimum damping value is an inertia-dependent expression $I_xL_p = 25(I_x)^{0.7}$ ft·lb·sec (sec. 3.6.1.1) which for the UH-1H computes to $L_p = -1.5$ sec^{-1} and is shown as the 8501A all-weather boundary in figure 1.

AGARD 577- Both damping (L_p) and sensitivity (L_δ) minimums are stated as ranges in this criteria document, which for forward flight are $-0.5 \leq L_p \leq -3$ sec^{-1} and $0.05 \leq L_\delta \leq 0.25$ rad/sec^2/in. The upper bounds of these minimum ranges are shown in figure 1.

MIL-F 83300- This criteria document provides a requirement in section 3.2.3.2 that can be translated to L_p and L_δ for hover and low speed (i.e., 35 knots and less) and a requirement in section 3.3.7.2 that can be translated into L_p in forward flight. Even though this experiment was flown at an airspeed of 60 knots (i.e., the low end of the forward flight range), the boundaries for both low-speed and forward flight are included in figure 1.

Configuration Setup and Validation

The approach used for configuration setup was in part a stability derivative match and in part a time-history match; it is outlined in detail in appendix A. Initial control-system gains were determined through use of a model-in-the-performance-index quadratic optimal program. These control gains were then programmed into the flight-control laws and each configuration was verified by checking the stability derivative generated on a ground simulator with the desired derivatives. In each case, it was found that only minor adjustments to the gains were necessary to achieve this match. Final adjustments were made in-flight through time-history matching with the desired roll-rate responses.

Figure 2 shows the resulting step responses for the uncoupled configurations of R2, R4, R6, and R8 at 60-knot level flight. Figure 3 shows the responses for the highly coupled configurations where $L_q/L_p = M_p/M_q = 0.5$; these configurations are designated as R2.5, R4.5, R8.5 (R6.5 was not included in this experiment). The coupling of pitch and roll rate can be clearly noted in these responses. Configurations with coupling ratios of 0.25 (i.e., R2.25, R4.25, and R8.25) were similarly configured but are not shown here.

Figure 4 shows the augmented pitch-step response with $M_q = -2$ sec^{-1} and the collective step response for the basic UH-1H; these characteristics remained constant throughout the experiment. The two yaw damped cases are also shown in this figure.

Task Definition

The task selected for this experiment was a near-terrain lateral maneuvering task involving a series of S-turns at constant altitude and speed. The task incorporated had many of the features of the NOE task used in the ground-simulation studies of references 1 and 2. However, an exact duplication of the ground-based simulation NOE task in the flight experiment was not possible because of safety and other practical considerations. Because of the single-engine height-velocity envelope for the UH-1H,

flying was restricted to heights above 80 ft. The selected course for the flight experiment is shown in figure 5. The task consisted of performing turns around the 1000-ft markers along runway 35 at Crows Landing NAS (Calif.). The pilots were instructed to maintain a reference speed of 60 knots and an altitude of about 100 ft; turns were to be made around imaginary piers extending up from the 1000-ft markers, and although it was not a true NOE task, it did prove sufficiently demanding to determine trends in handling qualities for the various configurations.

SYSTEM DESCRIPTION

This experiment was conducted with the NASA 733 UH-1H helicopter. Modifications were made to the helicopter flight control system, electrical and avionics systems, and cockpit panels and are referred to collectively as the VSTOLAND system. Figures 6 and 7 show an overall block diagram of that system and a cockpit layout. More detailed information on the system is provided in references 4 and 5.

Appendix B outlines the use of the system for this experiment, including details of the flight-control hardware, and treatment of the UH-1H stabilizer-bar dynamics.

RESULTS AND DISCUSSION

Results from this experiment are presented and discussed here in terms of pilot ratings, pilot commentary, frequency power (auto) spectral densities and statistical characteristics of specific aircraft states (i.e., maximums, minimums, averages, and standard deviations). Table 3 presents a summary of pilot ratings by the four pilots for all of the slalom runs. Results will be discussed first in terms of variations in damping and sensitivity and then in terms of pitch and roll cross-coupling; finally, the factors contributing to the results are interpreted.

Damping and Sensitivity

Figure 8 shows how averaged pilot ratings varied with roll sensitivity and damping for the configurations with increased yaw damping (N_r = -3.5 sec^{-1}). Also shown in this figure are data from the ground-based simulation studies of references 1 and 2, and flight data from the OH-6A and AH-1G, which were also flown over the same course. In addition, reference 6 provided data for the BO-105 from flight tests using one of the same pilots and a similar course. Of the number of handling-qualities criteria boundaries shown in figure 1, only those which in some way compare with the averaged data are shown in figure 8. These criteria include the MIL-H-8501A boundaries and the MIL-F-83300 low-speed boundaries. Both the MIL-F-83300 level 1 and level 2 and the MIL-F-8501A boundaries show some correlation with the data in the low-sensitivity and higher damping region. Likewise in the region of low damping and high sensitivity, some correlation exists with both the MIL-H-8501A all-weather boundary and the MIL-F-83300 level 2 boundary. Note that in the region of high damping and high sensitivity, the data from both flight and simulation show no clear trend and further study of that region is needed. Because of bounds on the flight-control system authorities, this experiment could not explore areas in the higher damping and sensitivity region and hence the potential of improved handling qualities in that region could not be assessed. The data does indicate a preference for a higher minimum level of damping

for this task, then cited by the criteria. Figure 9 summarizes some of the pilot comments in this experiment.

Pitch and Roll Cross-Coupling

Figure 10 shows the variation of pilot rating for the three roll-damping configurations L_p = -2, -4, and -8 sec^{-1} at three levels of pitch- and roll-rate coupling $L_q/L_p = -(M_p/M_q)$ = 0, 0.25, 0.5. Generally a degradation in pilot rating occurs at higher levels of coupling and is most notable for the high-damping case of $L_p = -8\ sec^{-1}$. At the higher coupling ratio the pilots noted an increased workload in controlling pitch and roll attitudes which in turn affected speed and height control. Previous studies (refs. 1, 7, 8) have indicated an upper bound on $L_q/L_p = -M_p/M_q$ of about 0.35 for minimum effect due to coupling, and these data more or less agree with that bound.

Figure 11 is a composite of the damping versus cross-coupling data for a fixed roll sensitivity (i.e., L_δ = 0.55 rad/sec^2/in.). Two observations are particularly noteworthy in this representation. The first is the already mentioned degradation in pilot rating for ratios of cross-coupling greater than 0.25; the second is the consistent improvement in pilot rating of from 0.5 to 1.5 ratings for the configurations with increased yaw damping. MIL-H-8501A places an all-weather minimum on yaw damping which is a function of moment of inertia I_z, and for the UH-1H inertia that minimum is $N_r = -1.7\ sec^{-1}$. This damping minimum is referenced to hover with no adjustments made for changes in damping as a function of speed. The two levels of yaw damping considered in this experiment were $N_r = -1.2\ sec^{-1}$ and $N_r = -3.5\ sec^{-1}$ as measured at 60 knots. Typical helicopter yaw damping increases with speed, and, for the UH-1H, the increase in N_r from hover to 60 knots is on the order of 0.6 sec^{-1}. For the two damping levels of this experiment the effects of speed would result in hover values of $N_r \cong -0.6\ sec^{-1}$ and $-2.9\ sec^{-1}$. Both the hover and 60-knot values of N_r bracket the MIL-H-8501A damping minimum of $N_r = -1.7\ sec^{-1}$ and indeed the data from this experiment indicate a significant improvement in handling qualities with the higher damping of $N_r = -3.5\ sec^{-1}$.

Frequency Analysis

A discussion of the frequency characteristics of certain helicopter interaxis coupling is given in reference 9. This reference shows that the pitch-roll coupling is not constant with frequency and in fact may have more than one frequency at which coupling is intensified. To assess this characteristic in the experiment, frequency-response tests were performed in flight by introducing computer-generated sinusoidal inputs into the pitch and roll controls. The results of these tests for the UH-1H manual mode (MAN) are shown in figures 12 and 13. These figures show the gain- and phase-frequency response for pitch and roll rates, as well as plots of the coupling ratios q/p and p/q. Note that the ratio plots indicate a significant frequency dependency; hence, placing a requirement on the steady-state value of coupling alone may not adequately constrain all the factors important to the pilot. To explore these frequency effects further, postflight analysis was performed to generate power (auto) spectral density plots of several flight variables. The results of this analysis, for several configurations are discussed below.

Figure 14 shows the autospectral density (ASD) plots for roll rate p and roll-control activity δ_ϕ of each of the pilots for an individual run of configuration MAN over the slalom course. All roll-rate plots show a consistency with the roll-cyclic plots and both show a dominance in spectral densities at frequencies below

1-1.5 rad/sec. For frequencies above 1 rad/sec, the roll-rate densities vary one from another, but all diminish to a negligible content at about 4 rad/sec. This is consistent with figure 13 which shows attenuation of roll-rate above 3-4 rad/sec.

Next, consider the ASD plots for pitch and roll response shown in figures 15(a) and 15(b). These results are for individual runs of the well-damped configurations R8, R8.25, and R8.5 which possess various levels of cross-coupling. As can be seen, these configurations also exhibit a dominant frequency band of pitch- and roll-rate and cyclic activity at less than 1.5 rad/sec, but in addition a secondary density emerges in both the pitch and roll axes at about 5 rad/sec, and increases in amplitude as the coupling increases (e.g., R8.25 and R8.5). By comparing figures 12, 13, 15(a), and 15(b) it can be seen that this higher frequency band occurs at a frequency where amplification occurs in the inherent UH-1H pitch-roll coupling. It is likely, then, that the secondary densities in figures 15(a) and 15(b) are vehicle-dependent in both frequency and amplitude. Since the measure of coupling use in this experiment is based on a steady-state value (i.e., zero frequency), any frequency dependency of this coupling, especially that which may be configuration-dependent, detracts from the generalization of the data. A survey of current helicopters or helicopter types might allow for at least a categorization of the frequency effects of coupling. Although not shown here, the same secondary-frequency band occurs for configurations R2.25, R2.5, R4.25, and R4.5.

One additional observation about this frequency analysis can be seen by comparing the density plots in figure 16, which are for the uncoupled configurations R2, R4, R6, and R8. First consider the plot for the lightly damped configuration R2. This spectrum exhibits a much broader low-frequency bandwidth for both roll rate and cyclic activity than is seen with the other configurations; moreover, the R2 configuration yields poorer pilot ratings, as shown in figure 8. This observation prompted a comparison of the dominant-frequency bandwidth for the uncoupled configurations to check for a possible correlation between bandwidth and handling qualities. To make this comparison, a measure of the half-power bandwidth ($B_{1/2}$) (ref. 10), is used. This measure is the bandwidth of the spectral density at one half of the peak density amplitude. Similarly, a quarter-power bandwidth $B_{1/4}$ is defined here for comparison with the half-power measures. Applying these bandwidth definitions to the plots of figure 16, as well as data from several other runs for each of the four pilots, results in the information shown in figures 17 and 18. First consider figures 17(a) and 17(b), which are plots of $B_{1/2}$ and $B_{1/4}$ versus roll damping, L_p, for all the runs; shown are the maximum, minimum and average values for the roll rate and roll cyclic responses, including data for the BO-105 from the tests of reference 10. These figures do indicate some correlation between bandwidth and roll-rate damping levels. Note, too, that the shapes of the plots for $B_{1/2}$ and $B_{1/4}$ are similar, implying some independence of where the bandwidth is measured. Now consider figure 18 which shows the same data in terms of pilot rating versus $B_{1/2}$. The advantage of this plot is that it is independent of L_p, and hence the basic UH-1H configuration (MAN) can also be included. This figure does indeed show a trend of improved pilot rating for the configurations with narrow half-power bandwidths. A more thorough study of this trend is needed, however, to determine whether it has any universal appeal for other vehicle types and control concepts (i.e., attitude-, rate-, and velocity-command system).

Statistical Survey of Data

A postflight statistical survey was conducted on several of the recorded variables to extract the maximum, minimum, mean, standard deviation, rms, and mean oscillation from each of the slalom runs. An example of the format for a single MAN run is

shown in table 4. Figures 19 and 20 graphically depict the maximum, minimum, mean and standard deviation for several runs of different configurations, all at the constant control sensitivity of $L_\delta = 0.55$ rad/sec^2/in. A noticeable feature of these data is the higher roll cyclic usage, as seen by δ_ϕ and σ_{δ_ϕ}, for the configurations R8, R8.25, and R8.5. This higher usage was noted by the pilots as insufficient control sensitivity. Apart from this observation, however, the data shows no trend with level of coupling or damping and, except for a slight tendency for the excursions of pilot A to be among the smaller, they show no appreciable difference between pilots. Furthermore, no correlation between pilot rating and these statistical measures can be cited. However, these measures do indicate a consistency with respect to excursions and activity on the slalom course, and this appears to be independent of control configuration. It is also worth mentioning that the statistical data indicated that control power was not a factor in this experiment since at no time were the control limits ($\delta_\phi = \pm 6.25$ in.) or servo limits (ASS = ±3°), which are not shown, exceeded.

CONCLUSIONS

The results presented here are for an in-flight simulation study of lateral helicopter handling qualities while performing a low-altitude lateral maneuvering task. During this study, variations were made to the vehicle roll damping, roll-control sensitivity, yaw damping, and pitch-roll cross-coupling. The task consisted of a series of S-turns which were flown at 60 knots and at an altitude of about 100 ft above the ground. Pilot rating data and statistical data were gathered and compared with several existing criteria and with the results of other comparable simulation studies. As a result of this experiment and the subsequent analysis, the following general trends and conclusions for the given task can be made.

1. An increase of yaw damping alone resulted in improved pilot ratings in all cases.

2. Flying-qualities trends for variations in roll damping and sensitivity for this 60-knot task agree well with portions of MIL-H-8501A and also with portions of MIL-F-83300 levels 1 and 2 criteria. However, for level 1 handling qualities the data indicate a need for much greater damping for performing such a task than is designated by the existing specifications.

3. Pitch-roll cross-coupling causes degraded pilot ratings when the steady-state ratios of M_p/M_q and L_q/L_p reach a high level of 0.5. Although this supports previous results, frequency analysis shows the coupling is frequency- and perhaps vehicle-dependent; hence, an additional dimension that goes beyond the derivative-ratio approach needs to be considered in specifying acceptable coupling.

4. A power spectral analysis of roll rate and roll-cyclic control activity for several configurations shows some correlation between the half-power bandwidth $B_{1/2}$ and both the roll damping (L_p) and pilot ratings. Further study is warranted to determine the general application of this trend.

5. A survey of the statistical measures of the maximum, minimum, means, and standard deviation of the variables p, δ_ϕ, q, δ_θ, u, h, and engine torque of all configurations for several runs indicate no appreciable correlation with pilot, configuration, or pilot rating.

APPENDIX A

CONFIGURATION SETUP AND VALIDATION

Initial modeling of the configurations for this experiment was achieved through a stability-derivative approach. The required SCAS gains for each configuration were determined by use of a model-in-the-performance-index quadratic optimization program which is outlined below.

Desired configuration:

$$\dot{X}_m = F_m X_m + G_m U_p \qquad \text{(where } U_p \text{ = pilots controls)}$$

$$Y_m = C_m X_m \qquad \text{(output vector)}$$

UH-1H vehicle:

$$\dot{X} = FX + GU \qquad \text{(where } U \text{ is defined below)}$$

$$Y = CX \qquad \text{(output vector)}$$

Case 1. Unaugmented UH-1H:

$$U = U_p$$

Case 2. Augmented UH-1H (i.e., VSTOLAND CSS mode):

$$U = KX + HU_p$$

where K, the feedback gain matrix, satisfies

$$J_{min} = \frac{1}{2} \int_0^\infty [(\dot{Y} - F_m Y)^T * Q * (Y - F_m Y) + (KX)^T * R * KX]dt$$

and H, the feedforward gain matrix, satisfies

$$E_{min} = (G_m * U_p - G * H * U_p)^T * S * (G_m * U_p - G * H * U_p)$$

Q, R, and S are weighting matrices

With the establishment of the matrices K and H, the individual gains can be easily programmed into the flight-control equation within the VSTOLAND airborne computer. The control laws used in this experiment are as follows.

It was found that most of the terms of the matrices K and H (i.e., the coupling feedforward and feedback) were not significant to this experiment and hence the control laws could be significantly reduced to the following equations.

Longitudinal Cyclic

$$B_{SS} = K_{\delta\theta}\left(\delta_\theta - \delta_{\theta_o}\right) + K_{q_B}\frac{s}{s + a_q}(q - q_o) + K_{p_B}\frac{s(p - p_o)}{s + a_p} + K_B\frac{(q - q_o)}{\tau_B s + 1}$$

$$\dot{B}_{PS} = K_{2_B} B_{SS}$$

where subscript o indicates the value of the state variable at system engagement.

Lateral Cyclic

$$A_{SS} = K_{\delta\phi}\left(\delta_\phi - \delta_{\phi_o}\right) + K_{p_A}\frac{s}{s + a_p}(p - p_o) + K_{q_A}\frac{s(q - q_o)}{s + a_q} + K_B\frac{(p - p_o)}{\tau_B s + 1}$$

$$\dot{A}_{PS} = K_{2_A} A_{SS}$$

Collective

$$C_{SS} = \hat{K}_{\delta_c}\left(\delta_{COL} - \delta_{COL_o}\right) - K_{\dot{h}_c}(w - w_o) + K_{q_c}\frac{s(q - q_o)}{s + a_q}$$

where $\hat{K}_{\delta_c} = K_{\delta_c} - C_1$ and $w = -\dot{h} + u \sin\theta$.

$$\dot{C}_{PS} = K_{2_C} C_{SS}$$

Directional

$$D_{SS} = \hat{K}_{\delta}\left(\delta_D - \delta_{D_o}\right) + K_{r_D}(r - r_o) + K_{p_D}\frac{1}{(\tau_p s + 1)}(p - p_o)$$

where $\hat{K}_{\delta_D} = K_{\delta_D} - C_2$

$$\dot{D}_{PS} = K_{2_D} D_{SS}$$

The terms C_1 (1.43 deg/in.) and C_2 (4.07 deg/in.) are included in the control equations to account for the control gearing of mechanical linkages which are retained at all times in collective and directional controls. These control equations were programmed in the VSTOLAND flight digital computer and the gains derived from the optimal procedure described above were implemented in these equations. Each configuration was verified on a ground simulator by matching stability derivatives and time-history responses. Final checkout, however, was conducted in flight, using time-history matching. Small variations in the "optimal" gains were required and easily made during these flights through a numerical keyboard

accessible to both pilots. An outline of the overall configuration verification procedure is shown in figure 21.

The resulting VSTOLAND control system gains used in the flight experiment are listed in table 5.

APPENDIX B

V/STOLAND AVIONICS AND FLIGHT CONTROL DESCRIPTIONS

The V/STOLAND digital avionics system was designed to provide navigation, guidance, control, and display functions and was installed on a UH-1H helicopter. For flight control studies, this system may be operated in a manual, control-stick steering (CSS), or autopilot (auto) mode with or without the flight director. In this experiment, both the manual and CSS modes were used, with the latter consisting of full fly-by-wire cyclic authority and limited authority in the pedals and collective controls. In the event of a malfunction, the V/STOLAND system reverts to the manual mode; also, either pilot can disengage the system at any time. A detailed description of the V/STOLAND system is presented in references 4 and 5.

Figures 6 and 7 show an overall block diagram of the V/STOLAND system and a cockpit layout, respectively. Figures 22-24 show the modifications to the flight-control system, which included the installation of four series and four parallel actuators. Unique electrohydraulic devices were integrated into the linkages between the research cyclic stick (co-pilot position) and the safety-pilot stick to allow the research stick to be disconnected for fly-by-wire pitch and roll control.

Data acquisition was provided by an on-board analog magnetic tape recorder and telemetered to a ground station for real-time monitoring and postflight analysis. Variables recorded included control positions, servo positions (both command and follow-up), attitudes, rates, accelerations, airspeed/altitude, V/STOLAND mode status, and calculated parameters. A description of the interface of the data-acquisition system with V/STOLAND is described in reference 11.

Stabilizer Bar Cancellation

An integral part of the UH-1H rotor system is the Bell stabilizer bar, which, as standard equipment, improves the basic vehicle handling qualities. At the onset of this program it was recognized that the effects of this device required careful consideration since the bar supplements the basic vehicle response in a manner which is undesirable for conducting variable-stability research. Research organizations using similar vehicles have resolved the problem by physically removing the bar; however, during this program an alternative approach was successfully implemented in which the bar's effects were cancelled through augmentation. This had the added advantage of providing a more desirable vehicle to revert to in the event of a research system failure.

The effect of the stabilizer bar is often mathematically modeled as a lagged pitch- and roll-rate feedback (or washout on attitude) which is added to the pitch- and roll-control acis equations (ref. 12) in the form of the following expressions:

$$B_{ICB}(s) = \frac{K_B}{\tau_B s + 1} q(s) \qquad \text{(pitch)}$$

$$A_{ICB}(s) = -\frac{K_B}{\tau_B s + 1} p(s) \qquad \text{(roll)}$$

The approach for this program was to cancel the above expressions through the stability and command augmentation system (SCAS) control equations. This was accomplished by programming the above expressions in the opposite sense, as shown in the previously stated control-law equations, and by adjusting K_B and τ_B in the simulator to achieve the desired cancellation via stability derivative and time-history matching. Final adjustments were made in flight; figure 25 shows a comparison of flight time-histories of roll rate for step inputs with and without stabilizer-bar cancellation and responses from other aircraft (e.g., ref. 13) where the stabilizer bar was physically removed. To approximate the physical removal of the stabilizer bar, values of $K_B = 0.554$ and $\tau_B = 2.3$ sec were required. As can be seen from figure 25, the bar-cancelled configuration yields a lightly damped ($L_p \cong -2$ sec^{-1}) first order response in angular rate and approximates the other two responses for the vehicles with the bar physically removed. The slight differences in these three responses can be attributed to the imperfect step inputs of the latter two cases. More importantly, however, these lightly damped responses depict a basic vehicle response which can be easily augmented to configurations of increased stabilization such as those in this study.

SCAS Servo Authority

An additional item of concern regarding system setup was that of adequate flight-control system servo authority. The configurations flown at the basic UH-1H sensitivity (i.e., $L_\delta = 0.55$ rad/sec^2/in.) were implemented through the pitch and roll cyclic fly-by-wire control system, utilizing the limited-authority series servo only. For these configurations, the series servo authorities of 26% in pitch and 29% in roll were adequate and thus at a constant speed of 60 knots, servo saturation was not a problem.

Configurations having varied control sensitivities, however, required the use of both the series and parallel servos to attain the required authority. During the V/STOLAND development phase the parallel servos were installed as rate servos to trim or off-load the faster series servos, but because of problems such as backlash and position sensing, the initial drive scheme could not be used with the control laws described above. To alleviate these problems a scheme of complementary filtering, as shown in figure 26, was used. This scheme, which was motivated by reference 14, uses a computed estimate and a measurement estimate of the parallel servo position to generate a supplement to the servo command. The parallel-servo gain K_2 was used to turn the parallel-drive scheme on and off.

REFERENCES

1. Chen, R. T. N.; and Talbot, P. D.: An Exploratory Investigation of the Effects of Large Variations in Rotor System Dynamics Design Parameters on Helicopter Handling Characteristics in Nap-of-the-Earth Flight. J. Am. Helicopter Soc., July 1978.

2. Chen, R. T. N.; and Talbot, P. D.: A Piloted Simulator Investigation of Augmentation Systems to Improve Helicopter Nap-of-the-Earth Handling Qualities. Paper 78-29, 34th Annual National Forum of the American Helicopter Society, May 1978.

3. Heffley, R. K.; et al.: A Compilation and Analysis of Helicopter Handling Qualities Data. Vol. I. NASA CR-3144, 1979.

4. Liden, S.: V/STOLAND Digital Avionics Systems for UH-1H. NASA CR-15279, 1978.

5. Baker, F. A.; Jaynes, D. N.; Corliss, L. D.; Liden, S.; Merrick, R. B.; and Dugan, D. C.: V/STOLAND Avionics System Flight-Test Data on a UH-1H Helicopter. NASA TM-78591, 1980.

6. Pausder, H. J.; and Gerdes, R. M.: The Effects of Pilot Stress Factors on Handling Quality Assessment during U.S./German Helicopter Agility Flight Tests. NASA TM-84294, 1982.

7. Huston, R. J.; and Ward, J. F.: Handling Qualities and Structural Characteristics of the Hingeless-Rotor Helicopter. NASA SP-116, 1966.

8. Garren, J. F., Jr.: Effects of Gyroscopic Cross-Coupling Pitch and Roll on the Handling Qualities of VTOL Aircraft. NASA TN D-812, 1961.

9. White, F.; and Blake, B. B.: Improved Method of Predicting Helicopter Control Response and Gust Sensitivity. Paper 79-25, 35th Annual National Forum of the American Helicopter Society, May 1979.

10. Bendat, J. S.; and Piersol, A. G.: Engineering Applications of Correlation and Spectral Analysis. John Wiley and Sons, 1980.

11. Davis, J. M.: Instrumentation Calibration Manual for UH-1H Helicopter with V/STOLAND Systems. NASA TM-78568, 1979.

12. Talbot, P. D.; and Corliss, L. D.: A Mathematical Force and Moment Model of the UH-1H Helicopter for Flight Dynamics Simulations. NASA TM-73254, 1977.

13. Beck, D. E.; Woodson, W. B.; and Carico, G. D.: Second Interim Report UH-1N Automatic Flight Control System Evaluation. NATC Report FT-78R-72, Nov. 1972.

14. Garren, J. F., Jr.; Niessen, F. R.; Abbott, T. S.; and Yenni, K. R.: Application of a Modified Complementary Filtering Technique for Increased Aircraft Control System Bandwidth in High Vibration Environment. NASA TM X-74004, 1977.

TABLE 1.- SUMMARY OF EXPERIMENTAL CONFIGURATIONS

Configuration	L_δ	L_p	M_δ	M_q	N_r	M_p/L_q	L_q/L_p
MAN[a]							
MAN*[a]							
SBO							
R2	Varied[b]	-2 sec^{-1}	0.17 $rad/sec^2/in.$	-2 sec^{-1}	-1.2 and -3.5 sec^{-1}[c]	0	0
R2.25	Fixed[d]	-2 sec^{-1}		-2 sec^{-1}	-1.2 and -3.5 sec^{-1}[c]	-.25	.25
R2.5	Fixed[d]	-2 sec^{-1}		-2 sec^{-1}	-1.2 and -3.5 sec^{-1}[c]	-.5	.5
R4	Varied[b]	-4 sec^{-1}		-2 sec^{-1}	-1.2 and -3.5 sec^{-1}[c]	0	0
R4.25	Fixed[d]	-4 sec^{-1}		-2 sec^{-1}	-1.2 and -3.5 sec^{-1}[c]	-.25	.25
R4.5	Fixed[d]	-4 sec^{-1}		-2 sec^{-1}	-1.2 and -3.5 sec^{-1}[c]	-.5	.5
R6	Varied[b]	-6 sec^{-1}		-2 sec^{-1}	-1.2 and -3.5 sec^{-1}[c]	0	0
R8	Varied[b]	-8 sec^{-1}		-2 sec^{-1}	-1.2 and -3.5 sec^{-1}[c]	0	0
R8.25	Fixed[d]	-8 sec^{-1}		-2 sec^{-1}	-1.2 and -3.5 sec^{-1}[c]	-.25	.25
R8.5	Fixed[d]	-8 sec^{-1}		-2 sec^{-1}	-1.2 and -3.5 sec^{-1}[c]	-.5	.5

[a] See Symbols list.
[b] See summary of results, figure 8.
[c] In the report, assume the value -3.5 sec^{-1} unless otherwise stated.
[d] Basic UH-1H sensitivity, L_δ = 0.55 $rad/sec^2/in.$

TABLE 2.- UH-1H STABILITY DERIVATIVE ESTIMATES[a]
(ref. 3)

	u	w	q	v	p	r	δ_{COL}	δ_{θ}	δ_{ϕ}	δ_{D}
X	-0.0244	0.0665	1.6142	0.0022	-1.1632	-0.2721	0.8087	0.8362	-0.0148	-0.0557
Z	.0123	-.8757	-1.6172	-.0235	-1.7359	1.9185	-11.5243	2.8179	-.0099	-.0383
M	.0032	-.0027	-.5230	.0009	.2043	.0131	.0125	-.1642	.9917	.9136
Y	.0010	-.0056	-1.2425	-.1248	-1.8915	1.5187	-.0798	.0504	.8756	1.9485
L'	-.0008	-.0061	-.7735	-.0160	-1.1266	.2915	-.0162	.0401	.5574	.5058
N'	-.0028	-.0149	-.0281	.0335	-.1946	-1.2827	.2098	.0575	.0790	-1.4287

[a] 60 knots, level flight at sea level, 8,000 lb, mid c.g.

TABLE 3.- PILOT OPINION DATA SUMMARY

Pilot	MAN	MAN*	SBO	L_δ	N_r	R2	R2.25	R2.5	R4	R4.25	R4.5	R6	R8	R8.25	R8.5
A	3,3,3, 3,3	3	4,4.5, 4	1.0×L_δ .75 1.0 1.5 2.0	-1.2 -3.5 -3.5 -3.5 -3.5	 6.5 5,5.5,6 4.0	 5,5.75	unflyable on slalom 6,6	 5 4,5,4,3.25,4 4.5	 5.25,4.5	 5.5,6	 3.5 5.0	5 4,6.5,5,5.5,4 4,4 4.5,5	 5,4.5	 6,7,8
B[a]	3,3,3, 3	4	4,3.5	1.0×L_δ .75 1.0	-1.2 -3.5 -3.5	4,6.5 5	5 3	 4	3.25,4.5 4	3 4,3.5	4.5 4.3.5		5,5.25,5 6	6 6	7 6.5
C[a]	3,3.5, 3,3	3	6,5,5	1.0×L_δ .75 1.0 1.5 2.0	-1.2 -3.5 -3.5 -3.5 -3.5	6.5 6 4.5,5,5.5 6.5	6.5 4,4.5	 6.5,5.5	4 4.5 3,4,3,3.5 3.5	6 3,5.5	5 5.5	 3 3.5	5.5 5,4,5.5,6,4.75 5,5 4,4.5	7 6	8 6.5,7.5
D[a]	4,3,3, 3,3	6.25,3	7,6.25 3.75	1.0×L_δ .75 1.0 1.25 1.5 2.0	-1.2 -3.5 -3.5 -3.5 -3.5 -3.5	5,7 4	6.25 6	 4	6.25 5,3.25	6.75 3	7.25 2.75,4	 3.25 3.25	7.25 5.75 7.5,5,6,4.25 3.5 4.5,3 4	7.25 5	7.75 7,6
Aver- age	3.1	3.8	4.8	1.0×L_δ .75 1.0 1.5 2.0	-1.2 -3.5 -3.5 -3.5 -3.5	5.8 6.25 5.0 5.25	5.9 4.7	8+ 5.3	4.5 4.75 3.9 4.0	5.25 4.1	5.6 4.5	 3.25 4.25	5.5 5.75 5.2 4.25 4.4	6.75 5.3	7.6 6.8

[a]These pilots also flew the OH-6A and Cobra (SCAS off) over the same slalom course; OH-6A, Pilot C PR = 3.0 and Pilot D PR = 3.0; Cobra (SCAS off), Pilot B Pr = 3.0 and Pilot D PR = 4.0.

TABLE 4.- UH-1H V/STOLAND SLALOM COURSE DATA STATISTICAL SUMMARY

Factor	Minimum	Maximum	Mean	Standard deviation	rms	Mean OSC
δ_ϕ, in.	-1.95	1.18	-0.59	0.79	0.98	15
A_{SS}, deg	.00	.00	.00	.00	.00	1497
$\dot{\phi}$, deg/sec	-16.83	18.97	-.52	8.51	8.52	22
ϕ, deg	-35.47	41.35	-.52	22.06	22.06	11
δ_θ, in.	-.95	.89	-.18	.36	.41	45
B_{SS}, deg	.00	.00	.00	.00	.00	1497
$\dot{\theta}$, deg/sec	-5.06	15.41	3.13	3.54	4.72	26
θ, deg	-3.16	8.68	2.54	2.15	3.33	22
v, ft/sec	87.13	109.86	99.05	4.66	99.18	22
δ_{COL}, in.	2.88	4.22	3.58	.33	3.60	20
C_{SS}, deg	.00	.00	.00	.00	.00	1497
$\dot{H}$, ft/sec	-4.83	6.88	.51	2.35	2.40	22
RALTF, ft	82.97	154.15	105.37	15.73	106.56	10
δ_D, in.	-5.61	-2.67	-4.33	.65	4.38	8
D_{SS}, deg	.00	.00	.00	.00	.00	1497
$\dot{\psi}$, deg/sec	-14.32	15.18	.09	6.45	6.44	26
ψ, deg	-41.26	17.37	16.54	20.03	25.97	8
TORPR1, lb/in^2	22.85	32.84	27.45	2.11	27.53	72
ACCYB1, g	-.01	.03	.01	.01	.01	36
ACCXB1, g	-.07	-.03	-.05	.01	.05	36
ACCZB1, g	-.06	.38	.10	.09	.13	22

TABLE 5.- SCAS CONTROL GAINS

Control gain	100% value	Configuration gains, percent										
		SBO	R2	R2.25	R2.5	R4	R4.25	R4.5	R6	R8	R8.25	R8.5
K_{q_B}	1.0 deg/deg/sec	0	36	36	36	36	36	36	36	36	36	36
K_{p_B}			5	10	18	5	12	20	5	5	20	25
$K_{\dot{h}_C}$												
K_{q_C}			5	5	5	5	5	5	5	5	5	5
K_{q_A}			0	-4	-7	-2	-7	-12	0	0	-8	-20
K_{p_A}			2	2	2	-6	-6	-6	-16	-27	-27	-27
K_{q_D}												
K_{p_D}			1	1	1	2	2	2	2	2	2	2
K_{r_D}			*a*									
K_{2_A}	.25 deg/sec/deg		*b*									
K_{2_B}												
K_{2_C}												
K_{2_D}												
K_B	.528	105	105	105	105	105	105	105	105	105	105	105
τ_B	3.3	70	70	70	70	70	70	70	70	70	70	70
K_{δ_θ}	1.85 deg/in.	100	100	100	100	100	100	100	100	100	100	100
K_{δ_ϕ}	1.59 deg/in.	100	*c*									
K_{δ_C}	1.43 deg/in.	100	100	100	100	100	100	100	100	100	100	100
K_{δ_D}	4.07 deg/in.	100	100	100	100	100	100	100	100	100	100	100
a_q	.167 sec	100	100	100	100	100	100	100	100	100	100	100
a_p	.5 sec^{-1}	100	100	100	100	100	100	100	100	100	100	100
τ_p	.5 sec	100	100	100	100	100	100	100	100	100	100	100

[a] The values for low and moderate damping were K_{r_D} (0→Nr=-1.2, -20→Nr=-3.5); and remained the same for columns R2 through R8.5.

[b] K_{2_A} = 0% (i.e., parallel servo off) for K_{δ_ϕ} = 100%; K_{2_A} = 100% (i.e., parallel servo on) otherwise.

[c] The value for K_{δ_ϕ} was varied from 75% to 200% for sensitivities of 0.41 to 1.1 $rad/sec^2/in.$

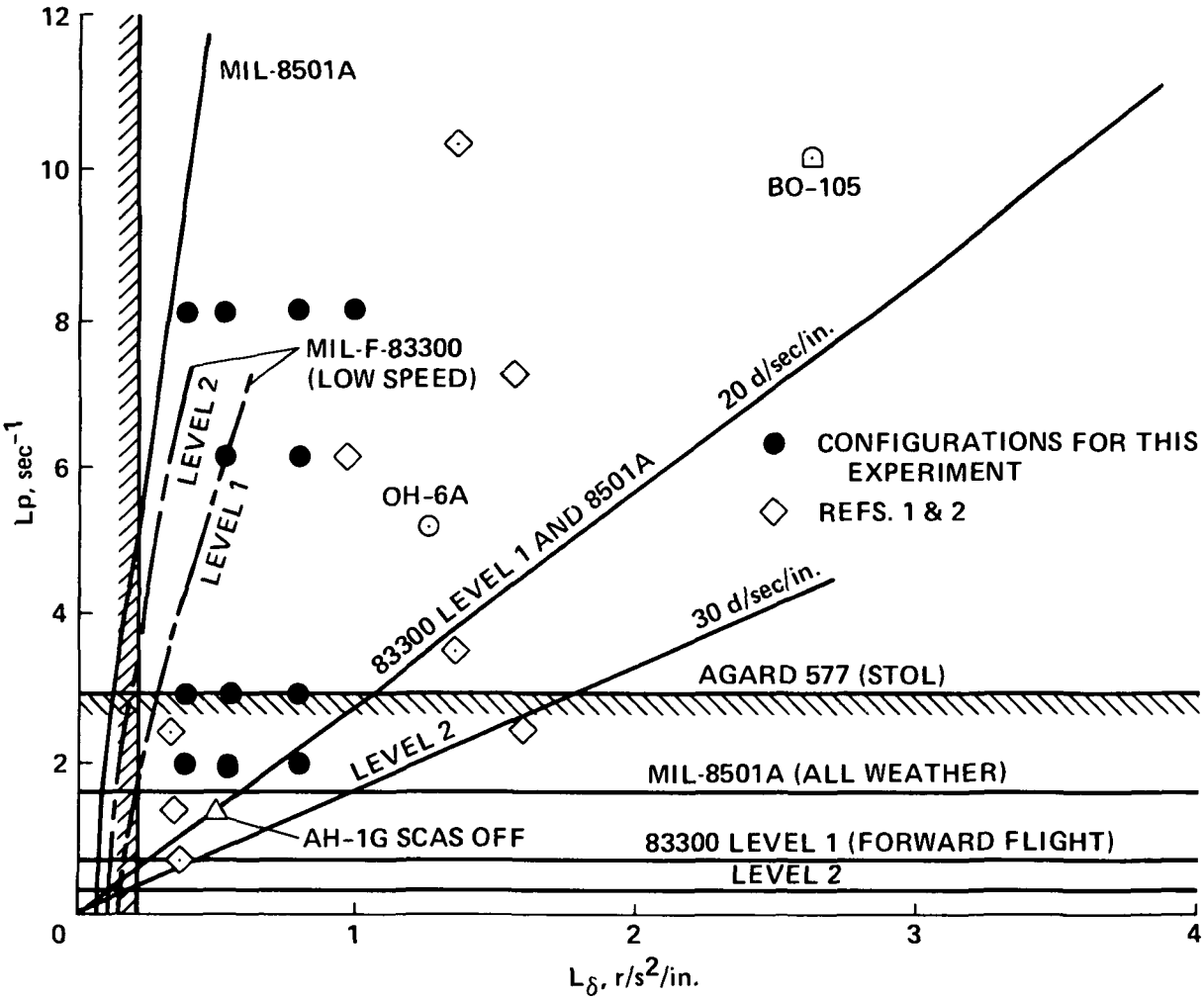

Figure 1.- Current flying qualities boundaries for roll control.

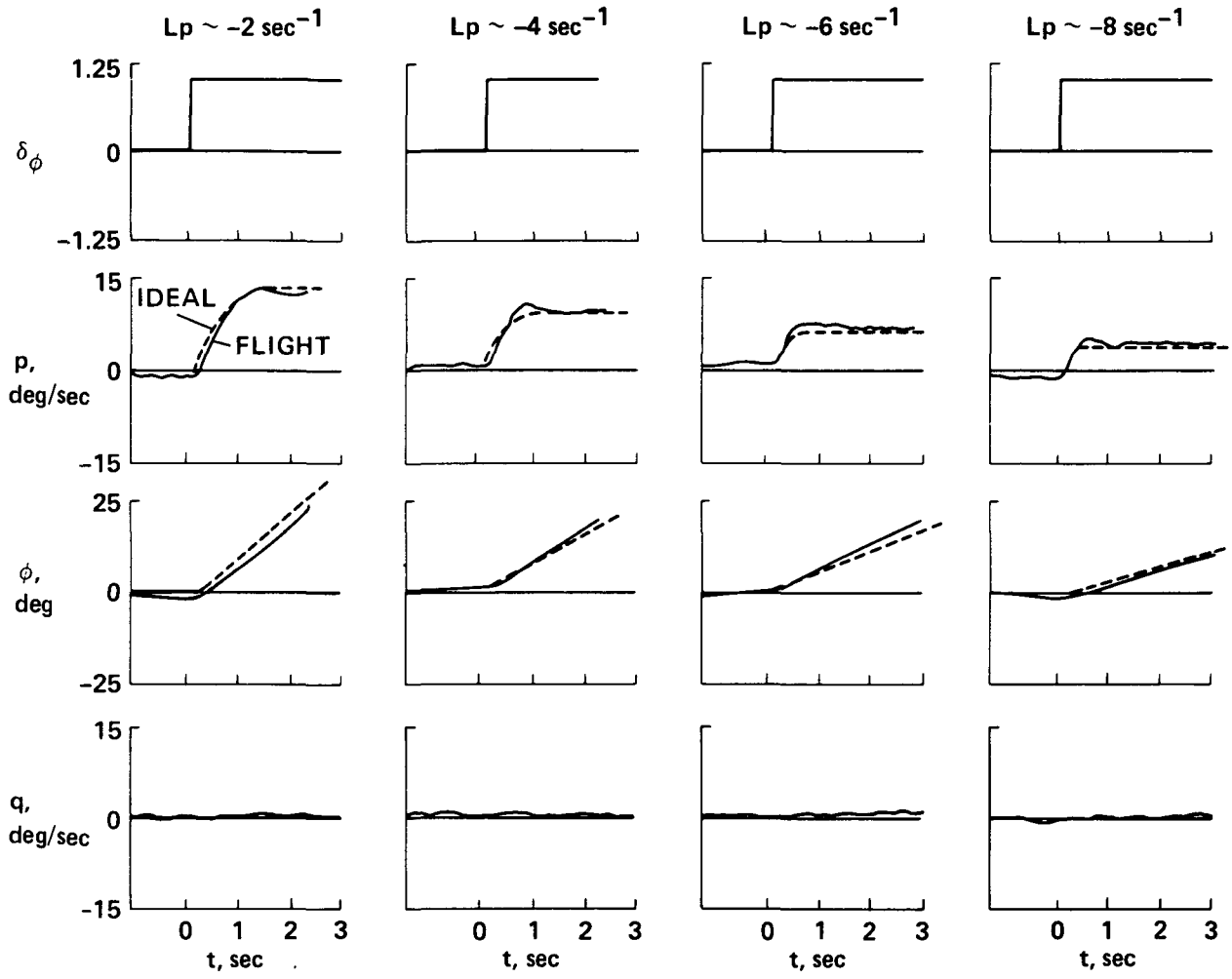

Figure 2.- Configuration verification responses-roll axis (60 knot flight data).

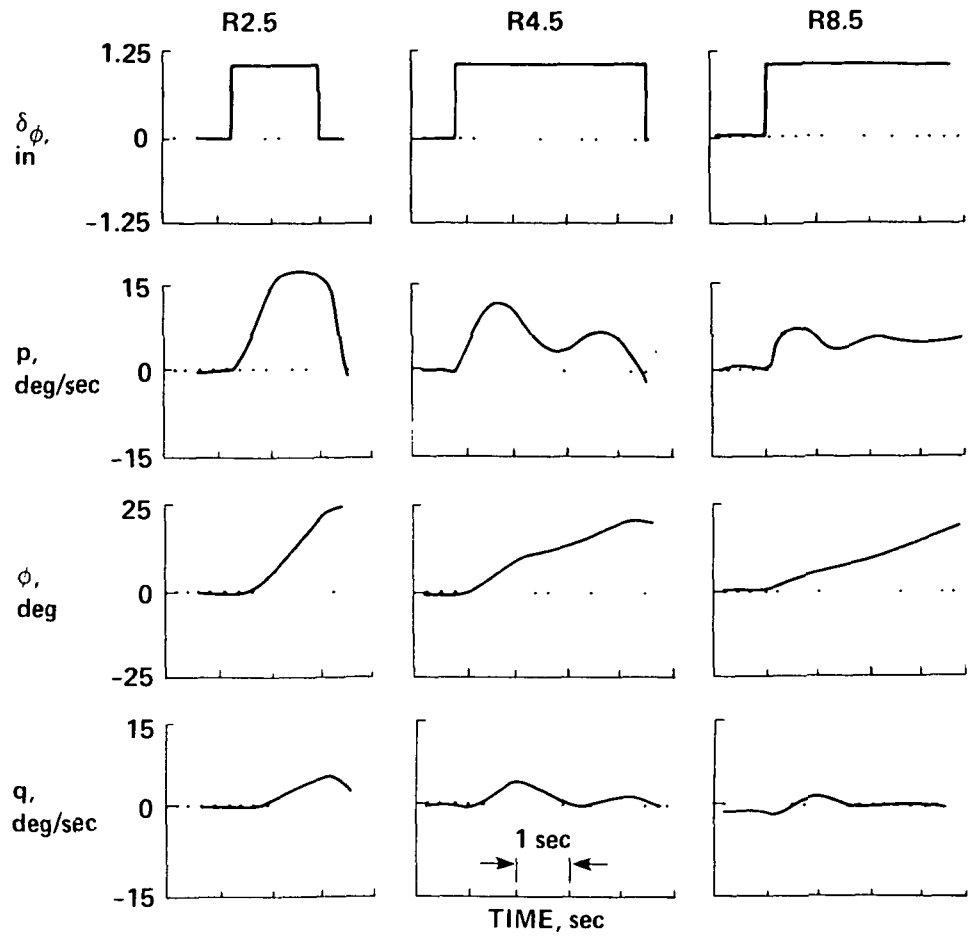

Figure 3.- Coupled responses-roll axis (60 knot flight data).

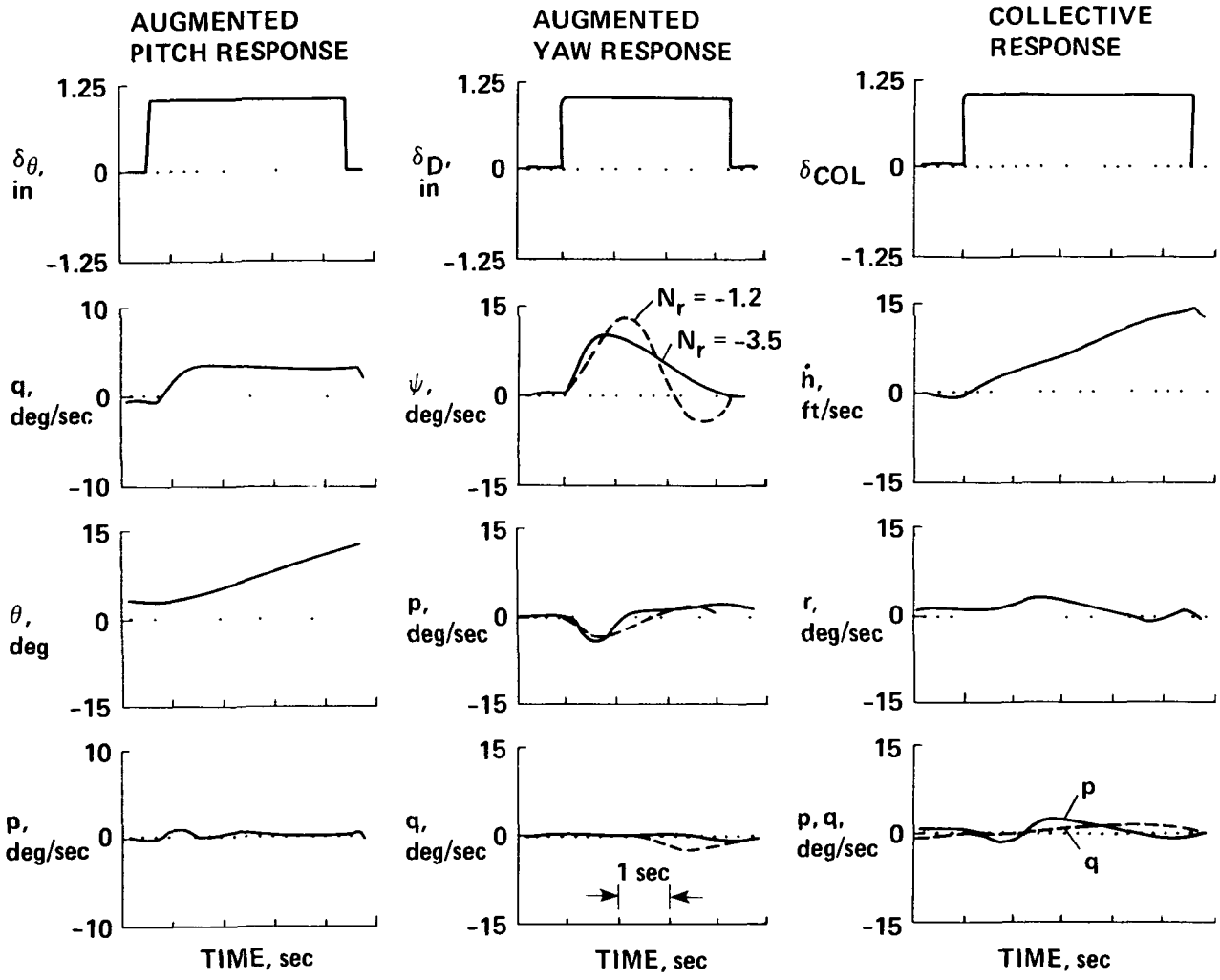

Figure 4.- Pitch, yaw, and collective responses (60 knot flight data).

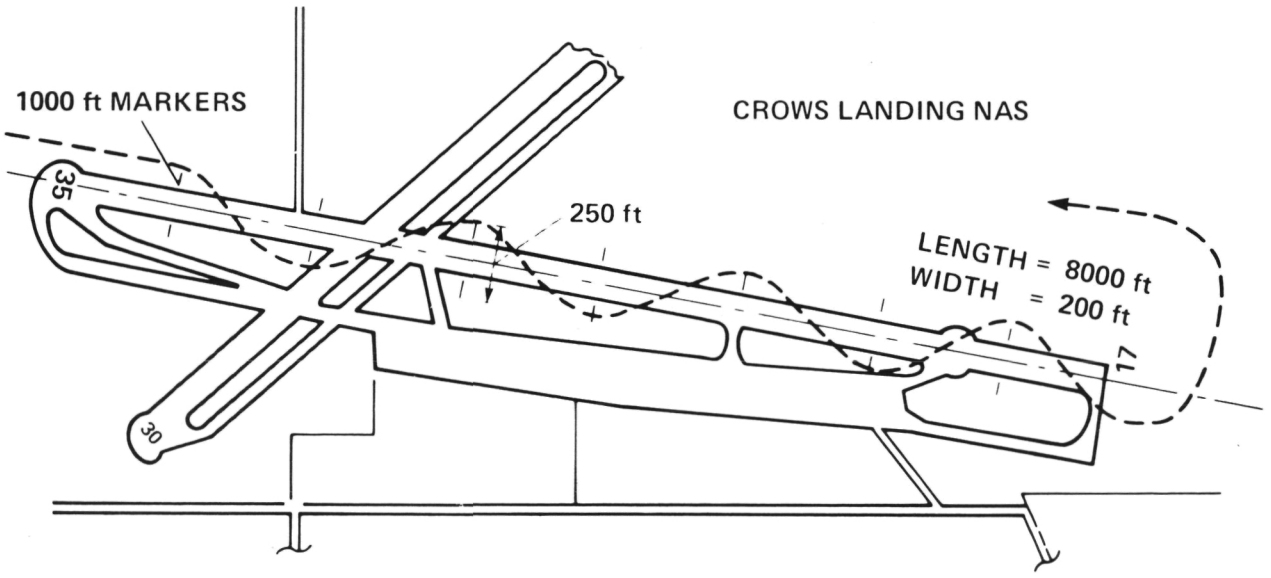

Figure 5.- Slalom-course task.

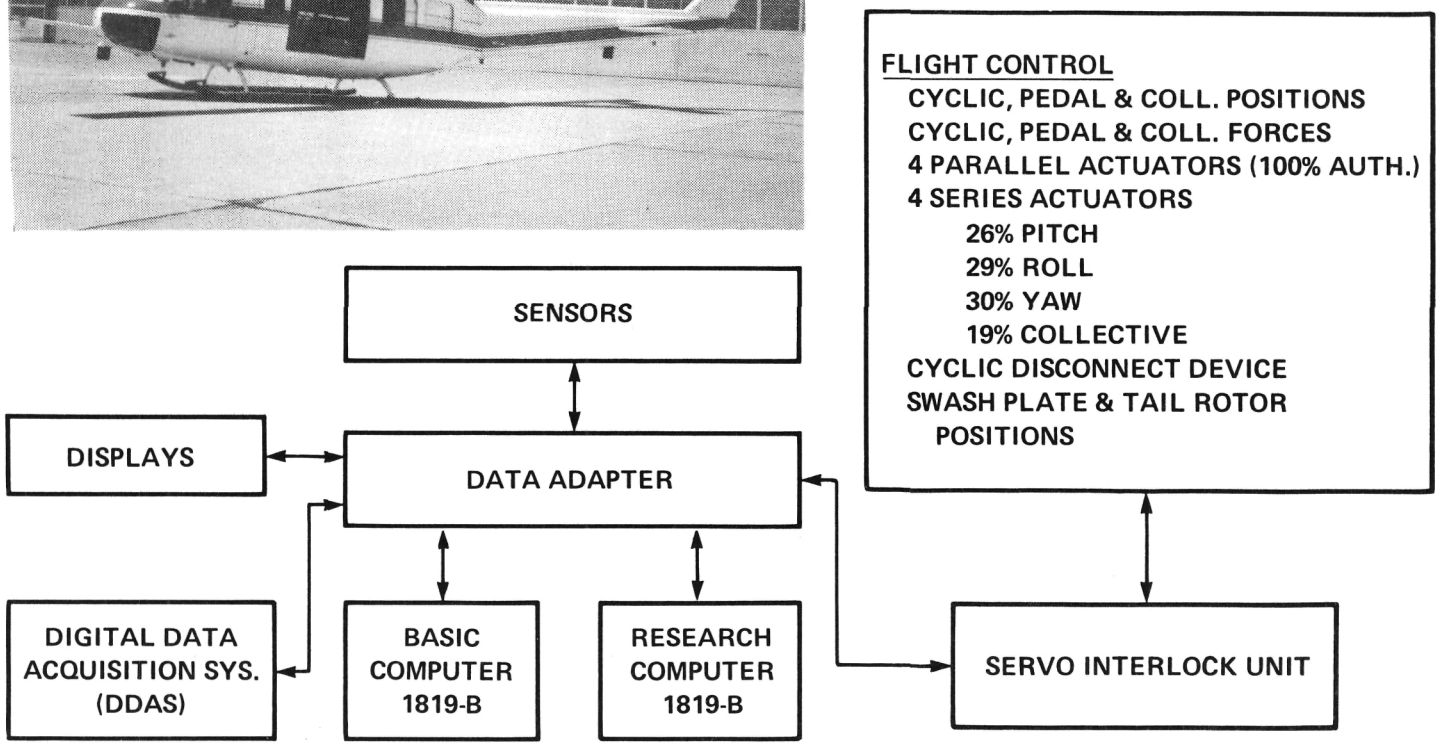

Figure 6.- UH-1H VSTOLAND system block diagram.

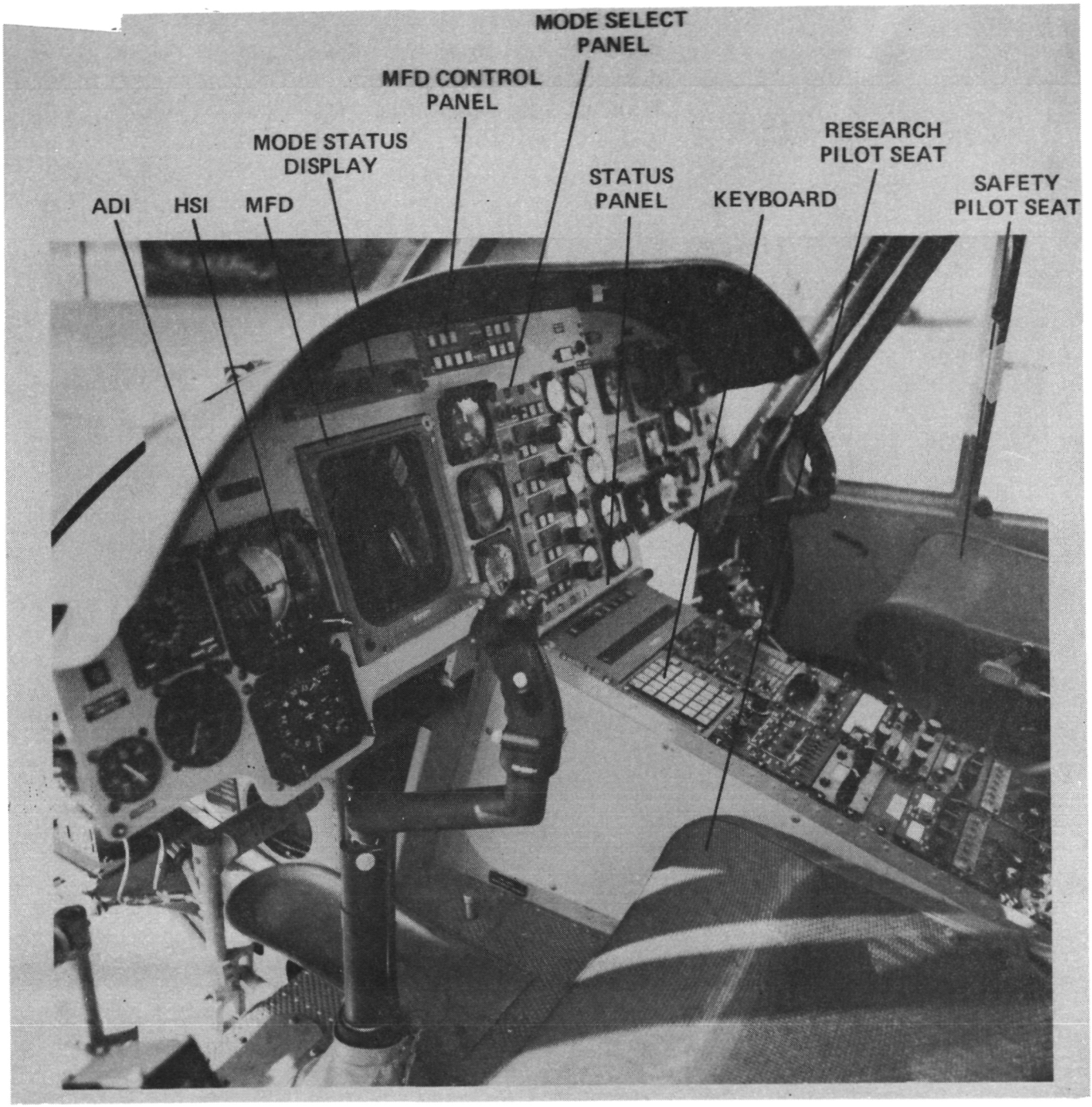

Figure 7.- Cockpit layout from research pilot's side.

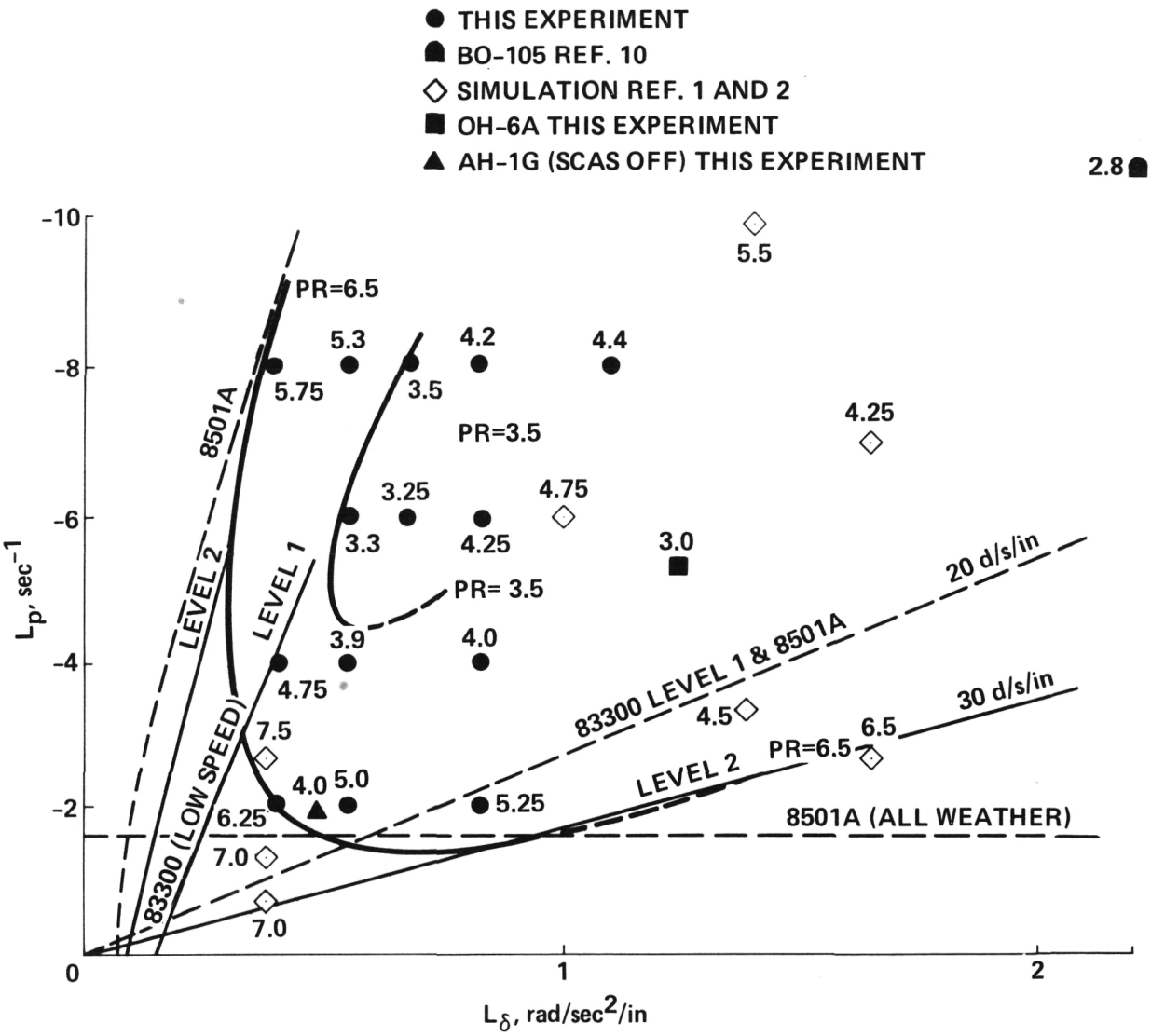

Figure 8.- Pilot rating results for roll control sensitivity and damping, 60 knots.

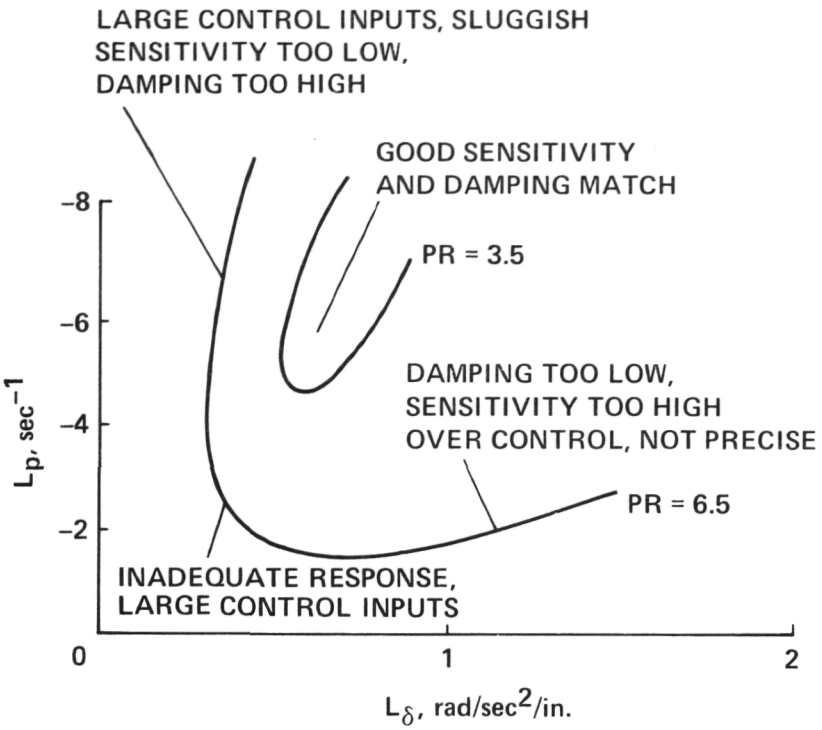

Figure 9.- Summary of pilot comments.

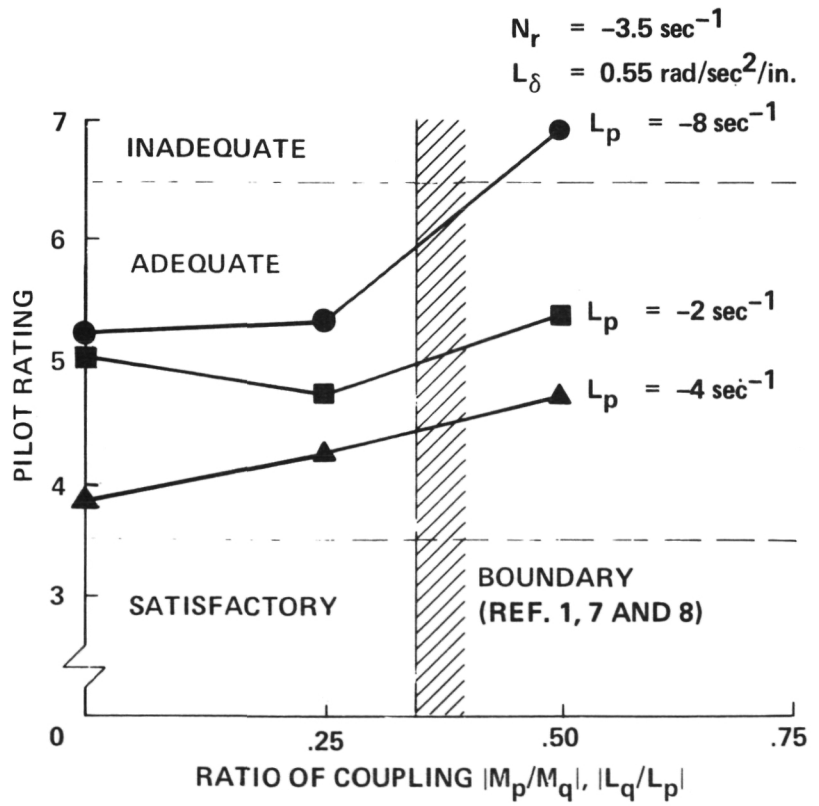

Figure 10.- Trends in pilot rating with ratio of coupling.

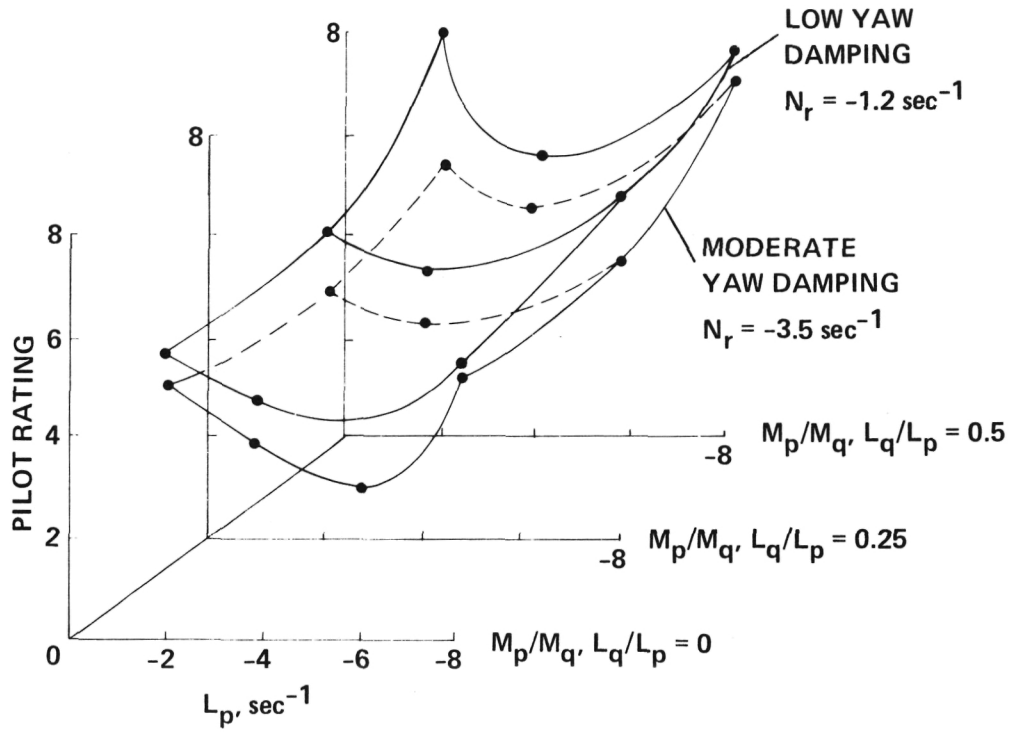

Figure 11.- Composite of roll damping and cross-coupling data.

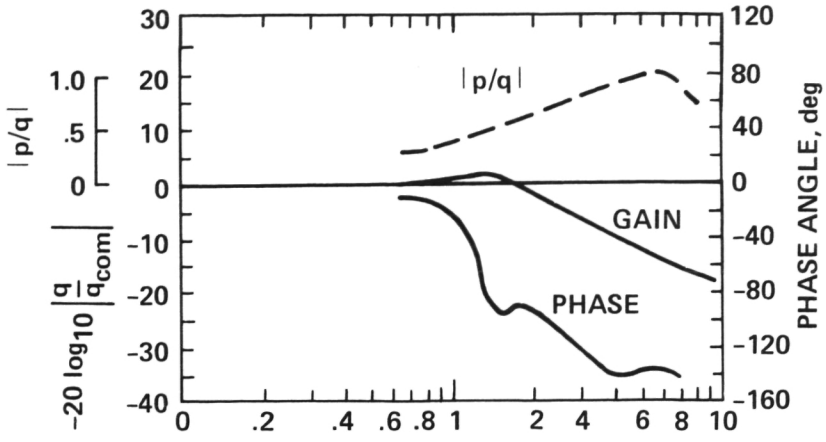

Figure 12.- UH-1H pitch frequency response, 60 knots.

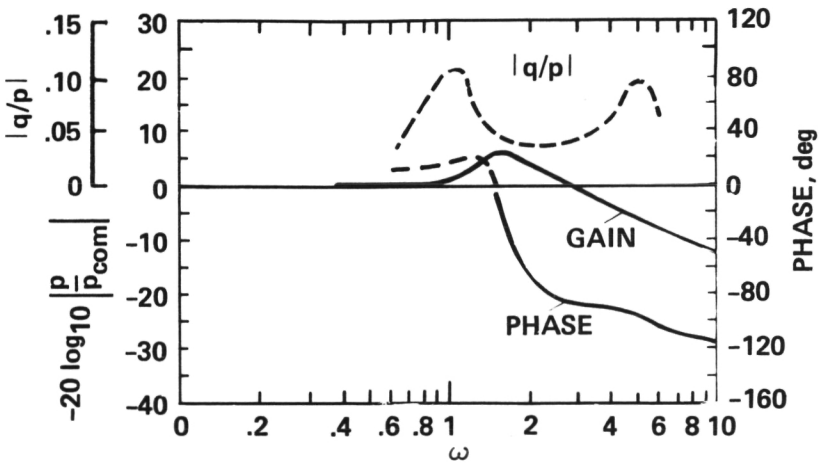

Figure 13.- UH-1H roll frequency response, 60 knots.

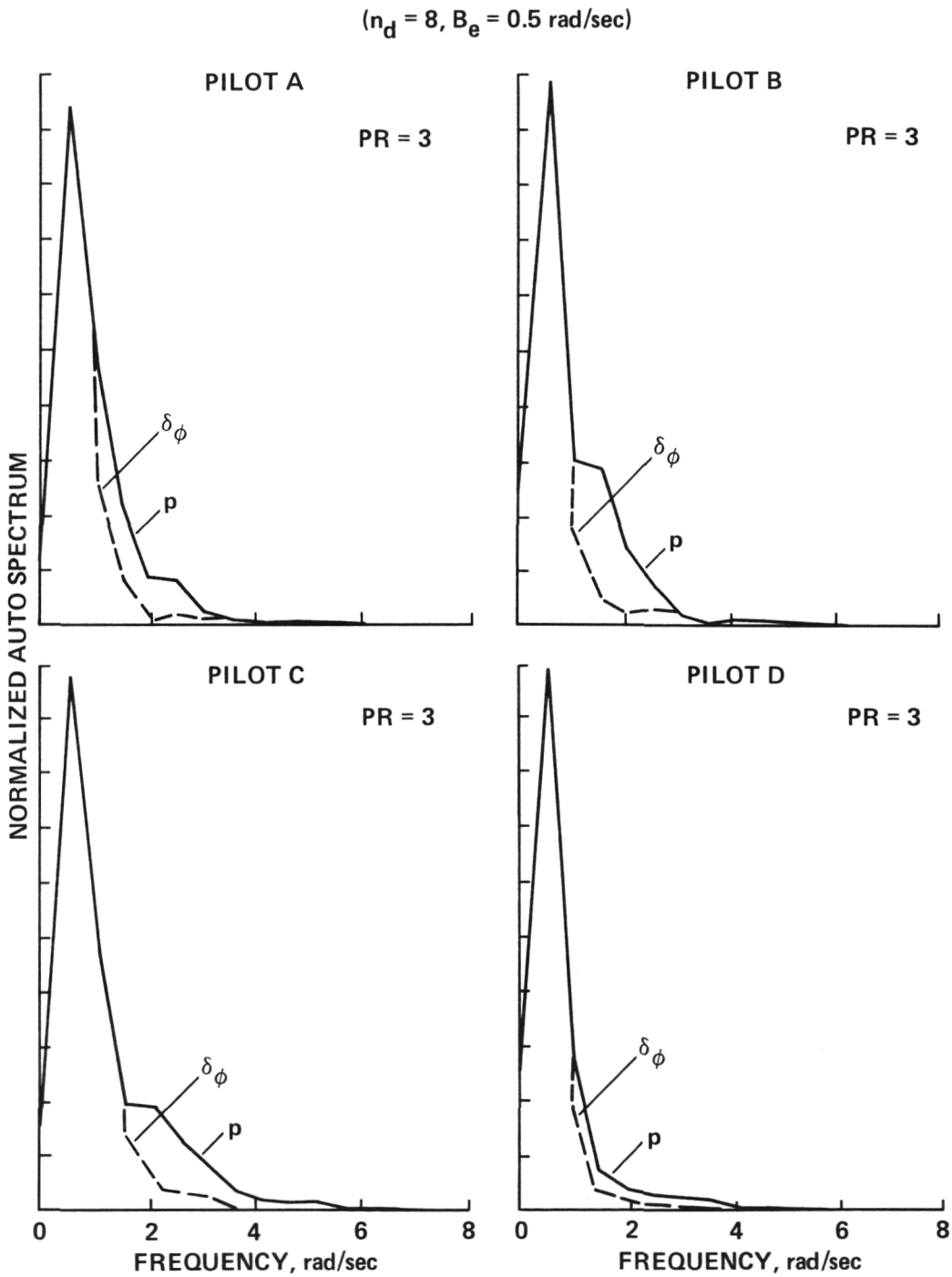

Figure 14.- Manual mode autospectral densities for roll rate and lateral cyclic.

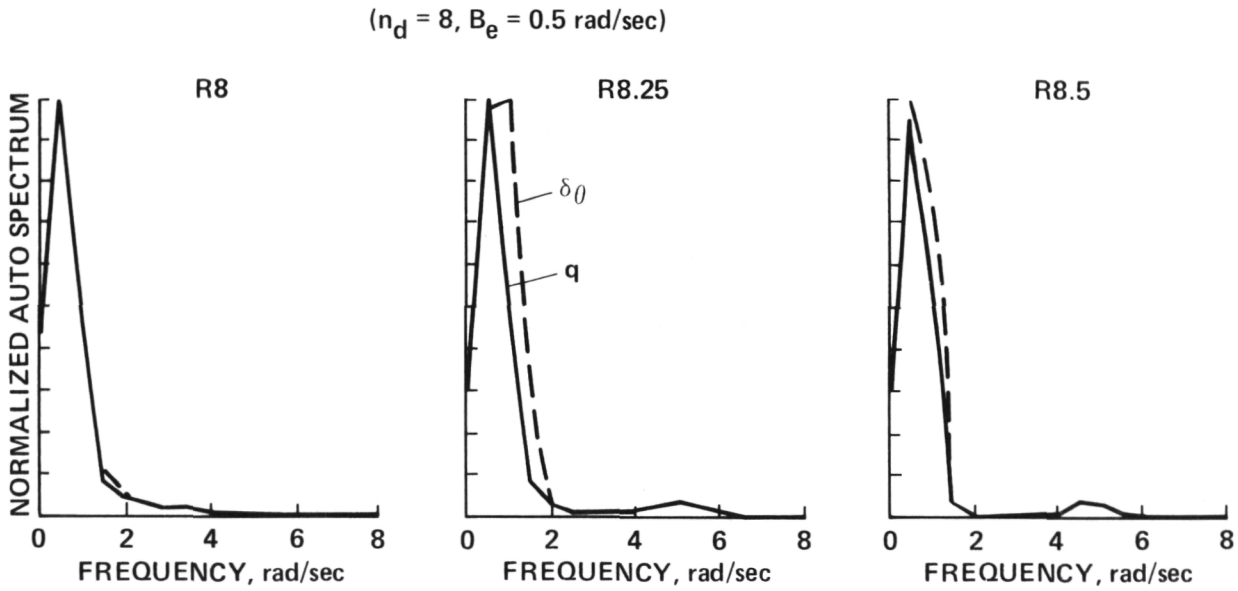

(a) Pitch autospectral densities for pitch rate and longitudinal cyclic.

Figure 15.- Configurations R8, R8.25 and R8.5.

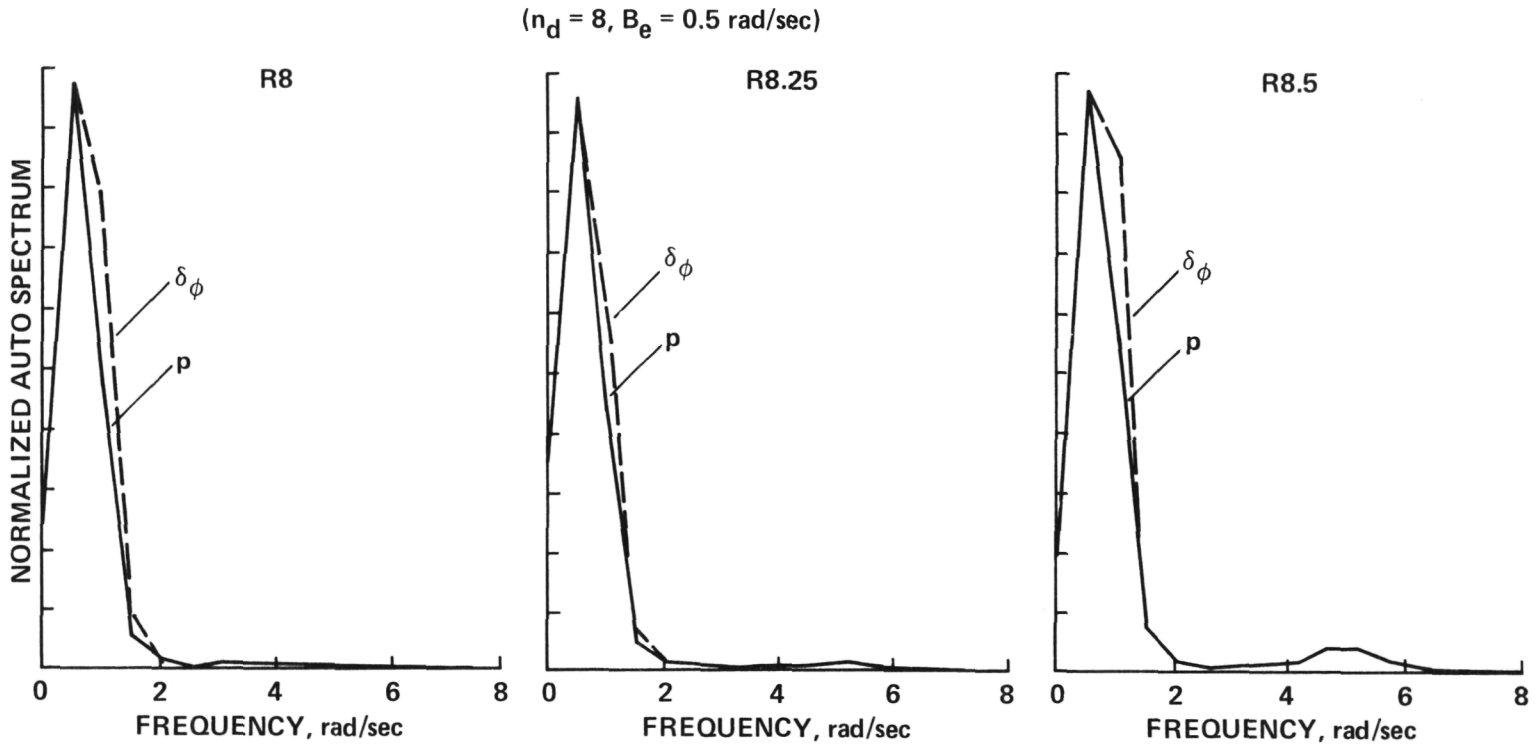

(b) Roll autospectral densities for roll rate and lateral cyclic.

Figure 15.- Concluded.

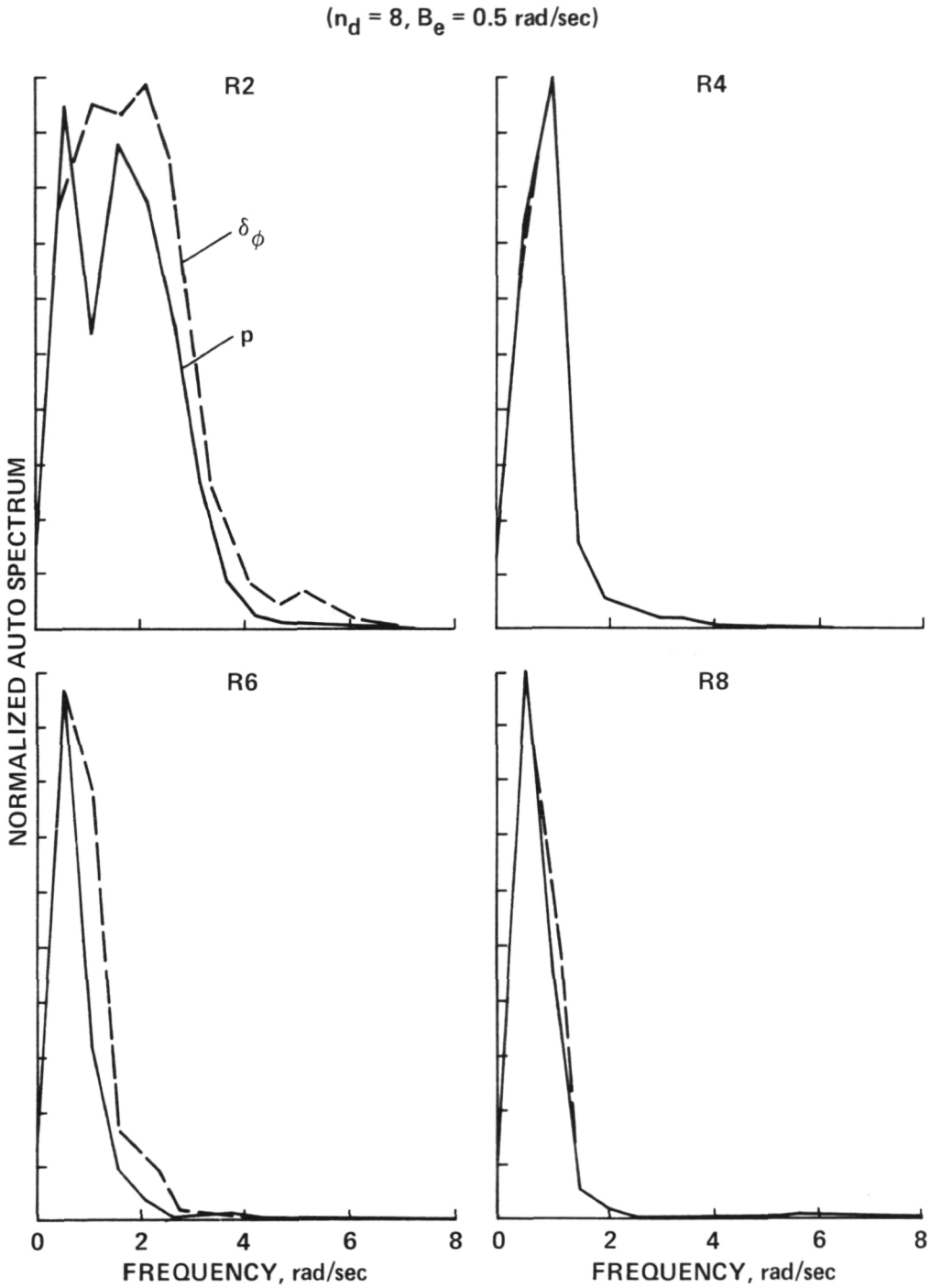

Figure 16.- Roll autospectral densities, configurations R2, R4, R6, and R8.

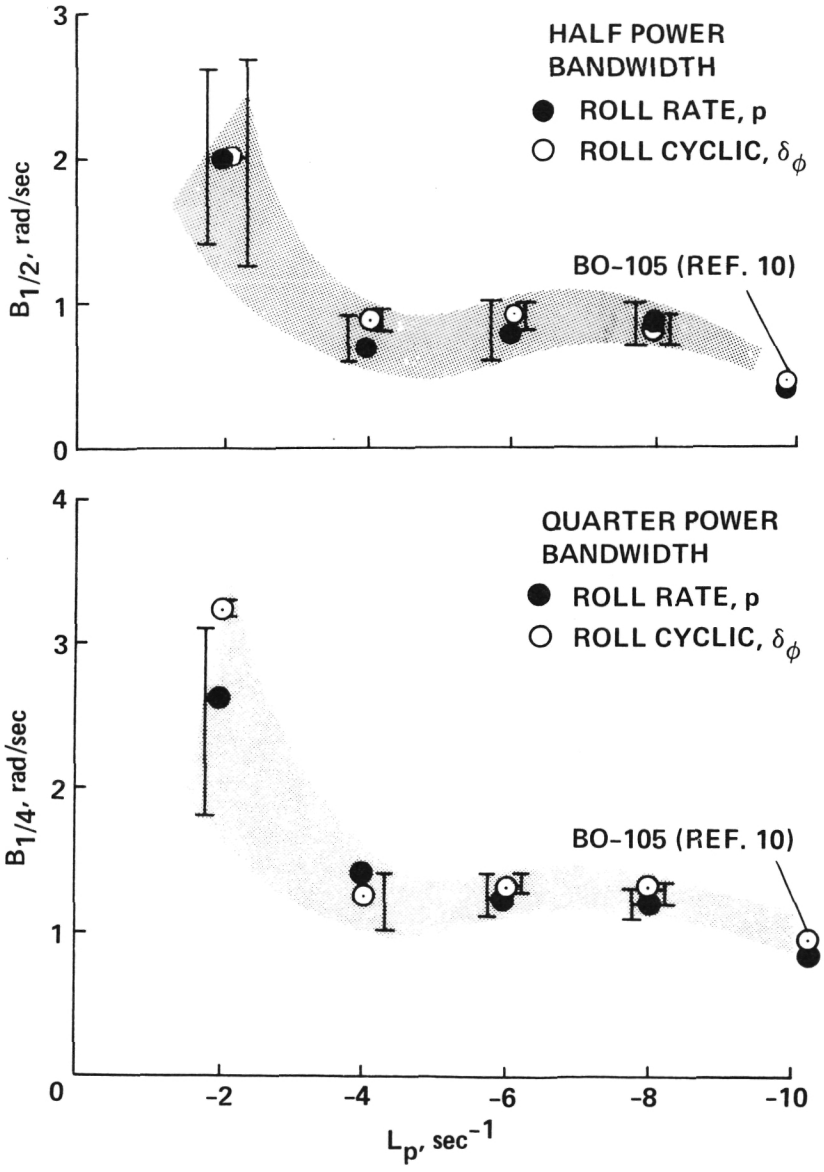

Figure 17.- Roll spectral density, bandwidths.

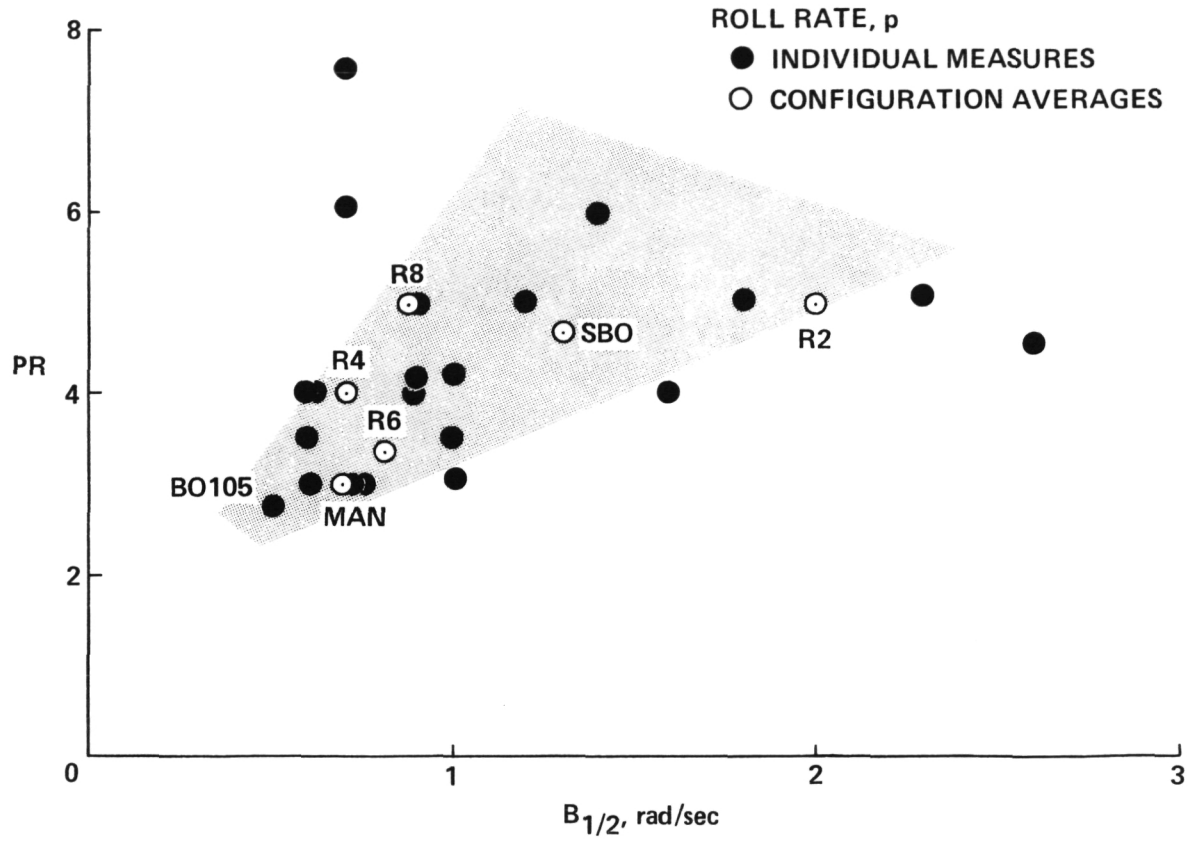

Figure 18.- Roll rate half power bandwidth versus pilot rating.

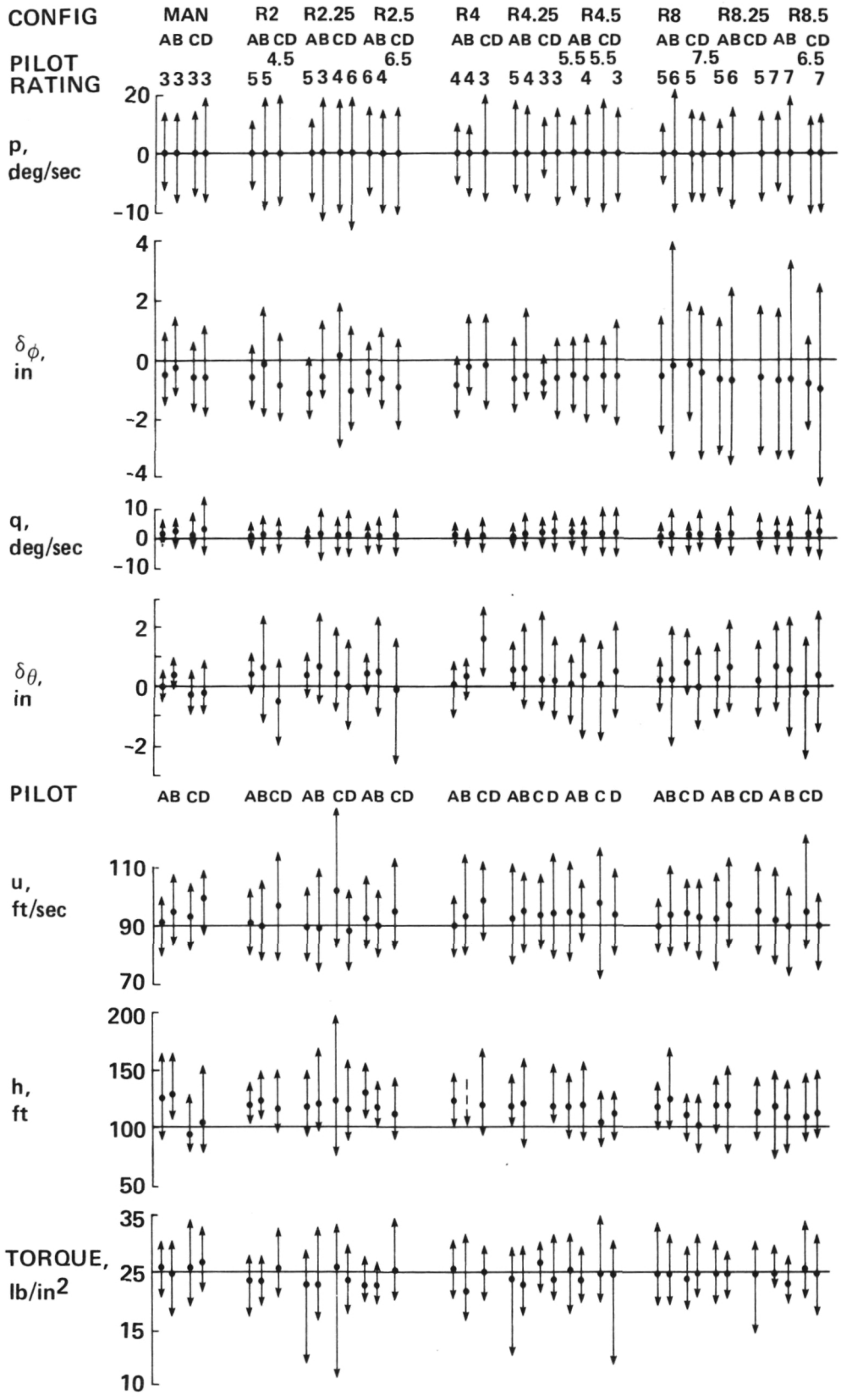

Figure 19.- Maximum, minimum, and average value summary.

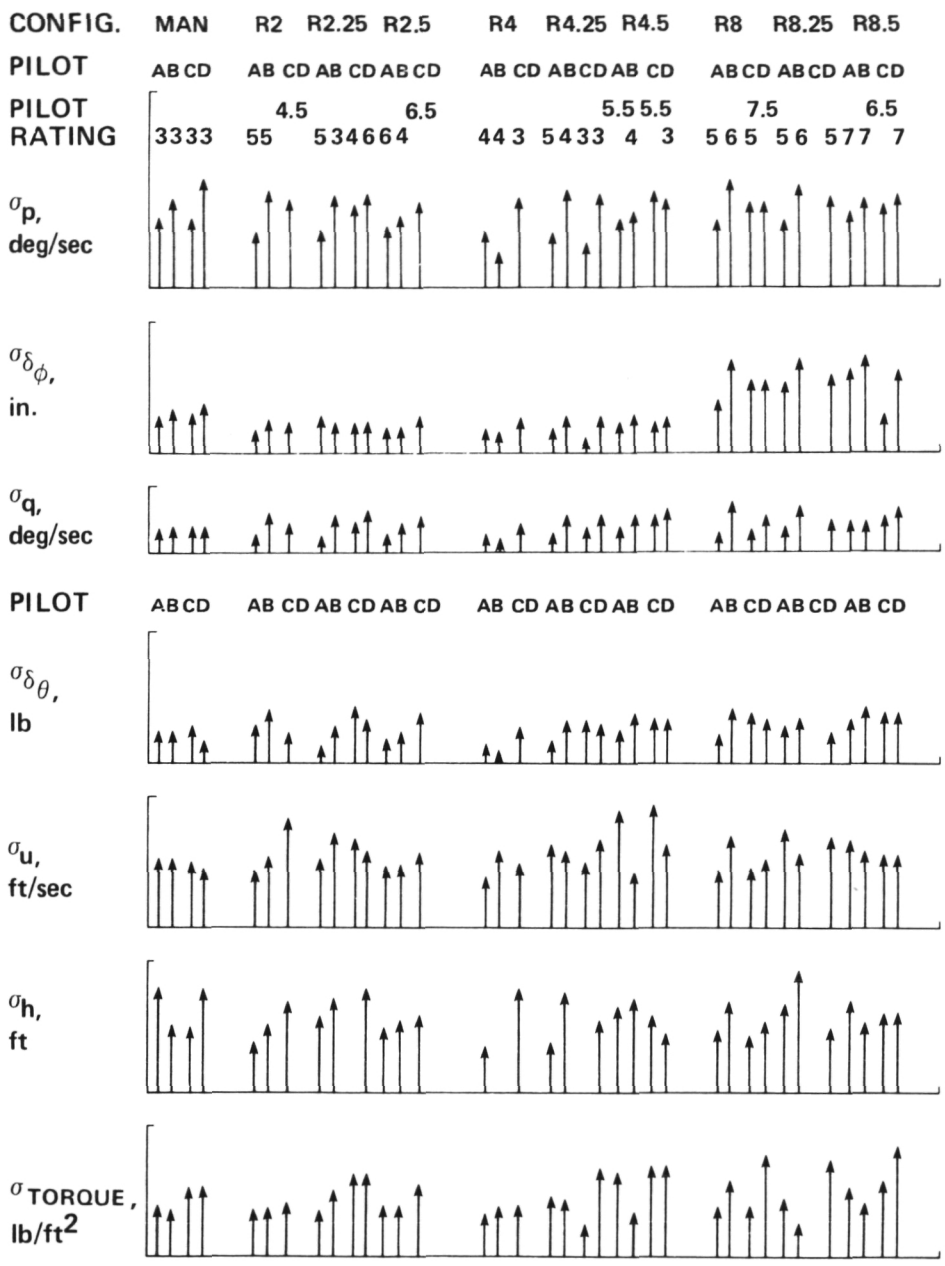

Figure 20.- Standard deviation summary.

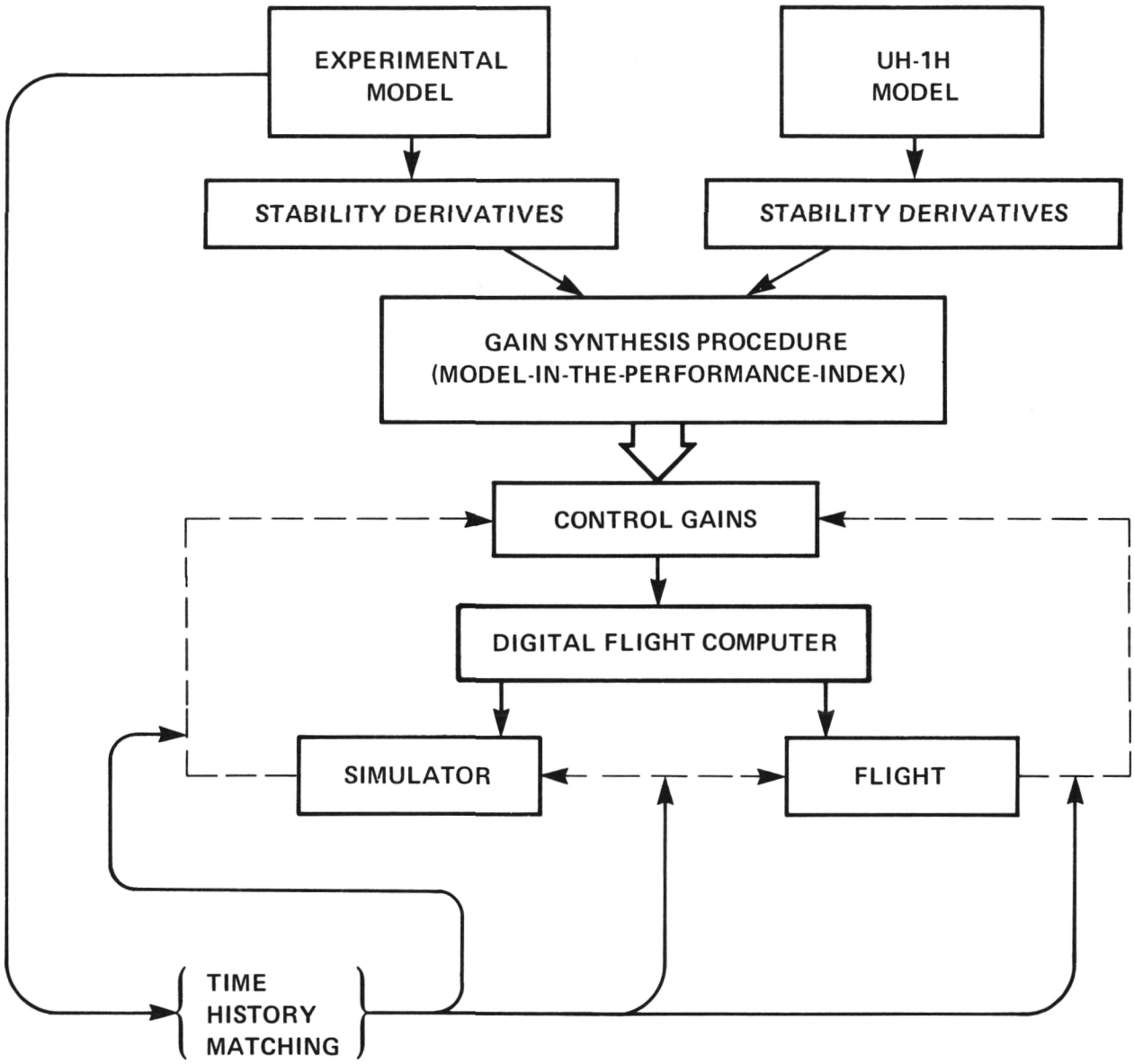

Figure 21.- Configuration verification cycle.

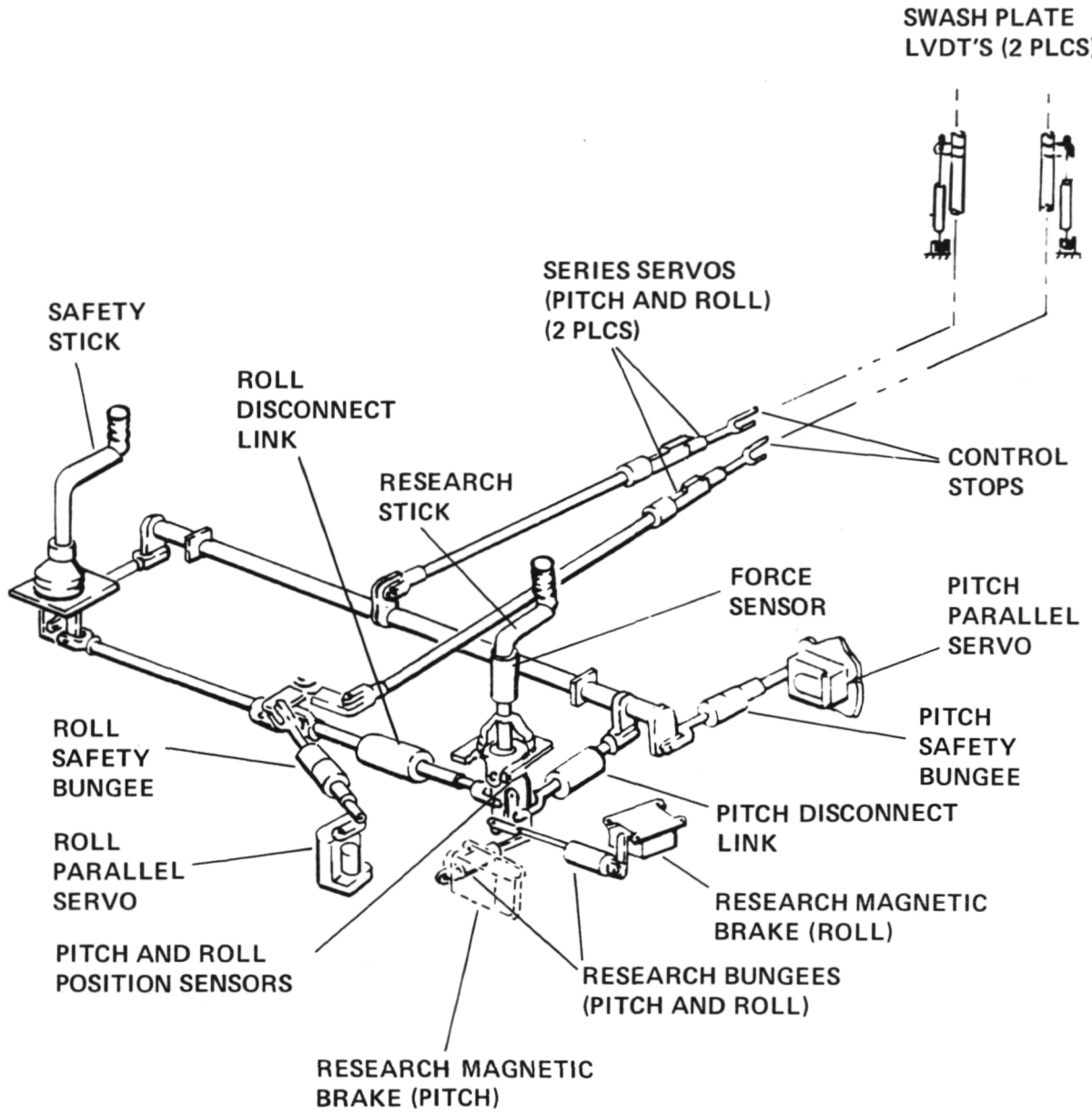

Figure 22.- UH-1H VSTOLAND cyclic controls.

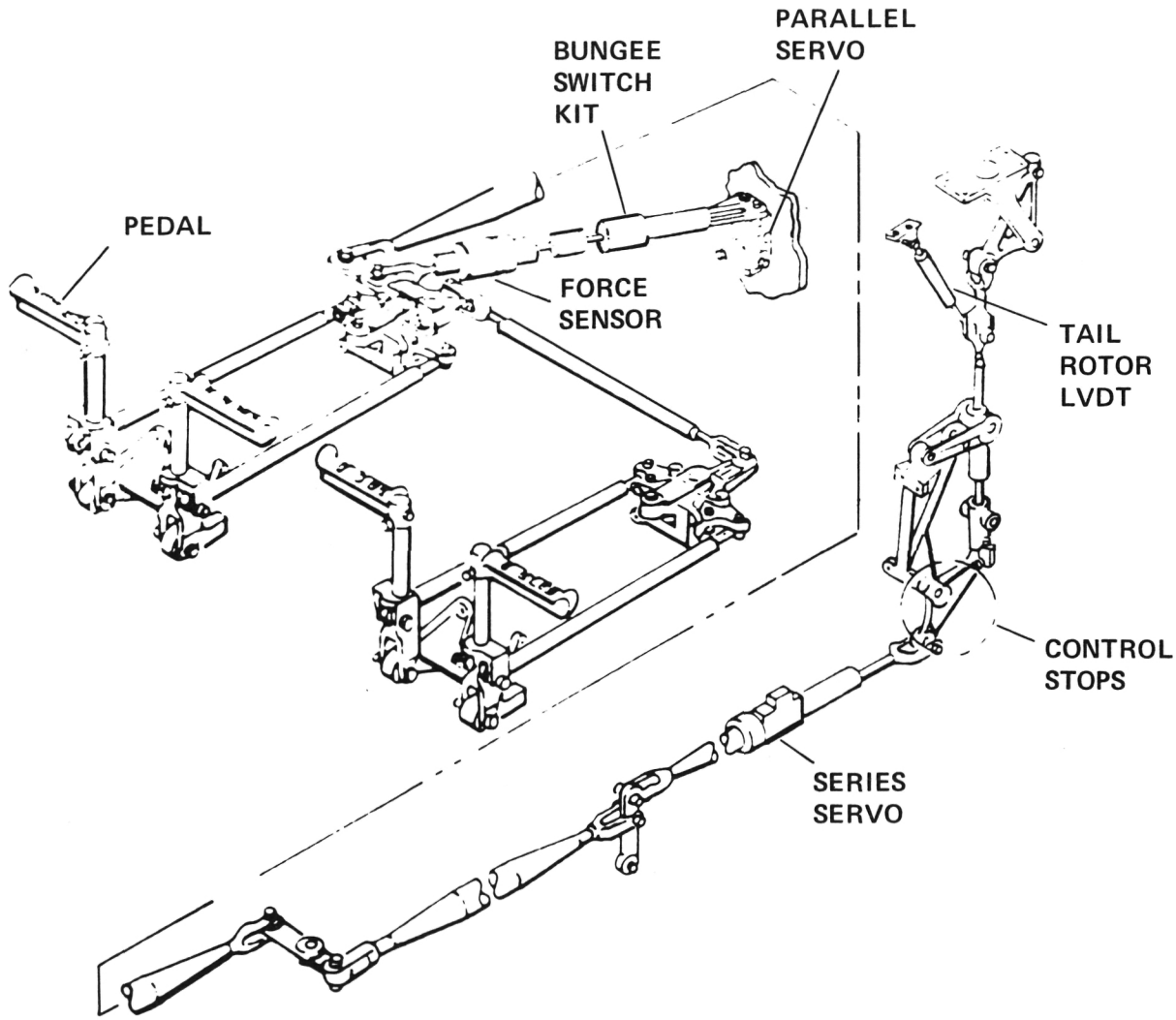

Figure 23.- UH-1H VSTOLAND directional controls.

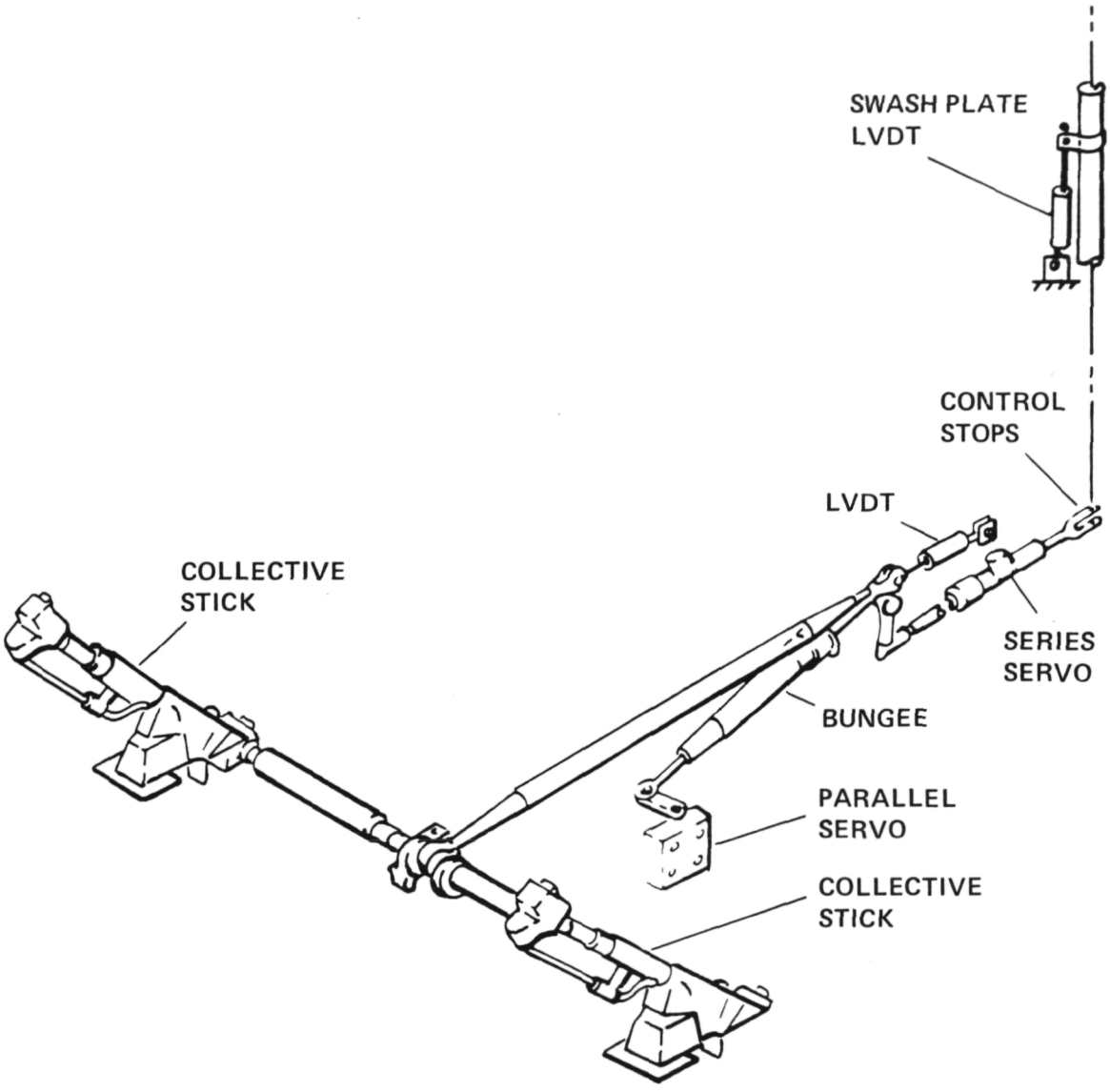

Figure 24.- UH-1H VSTOLAND collective controls.

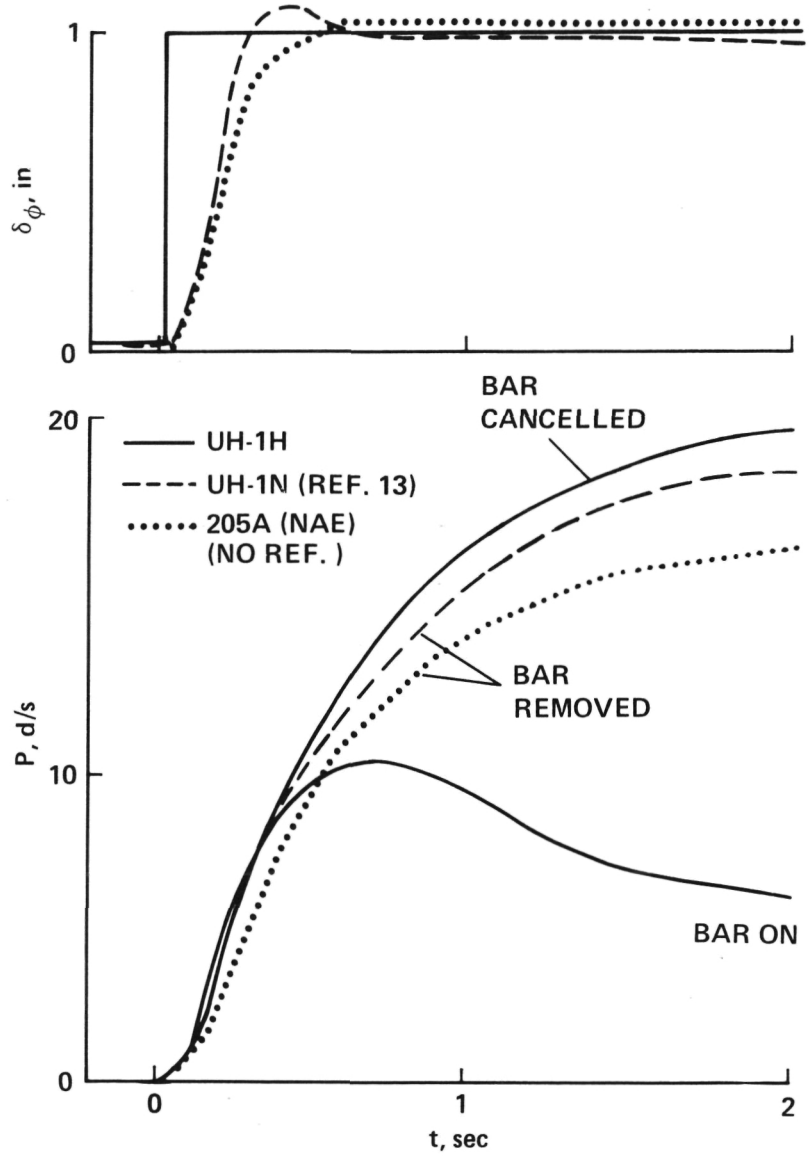

Figure 25.- Illustration of stabilizer bar cancellation-roll response to cyclic step.

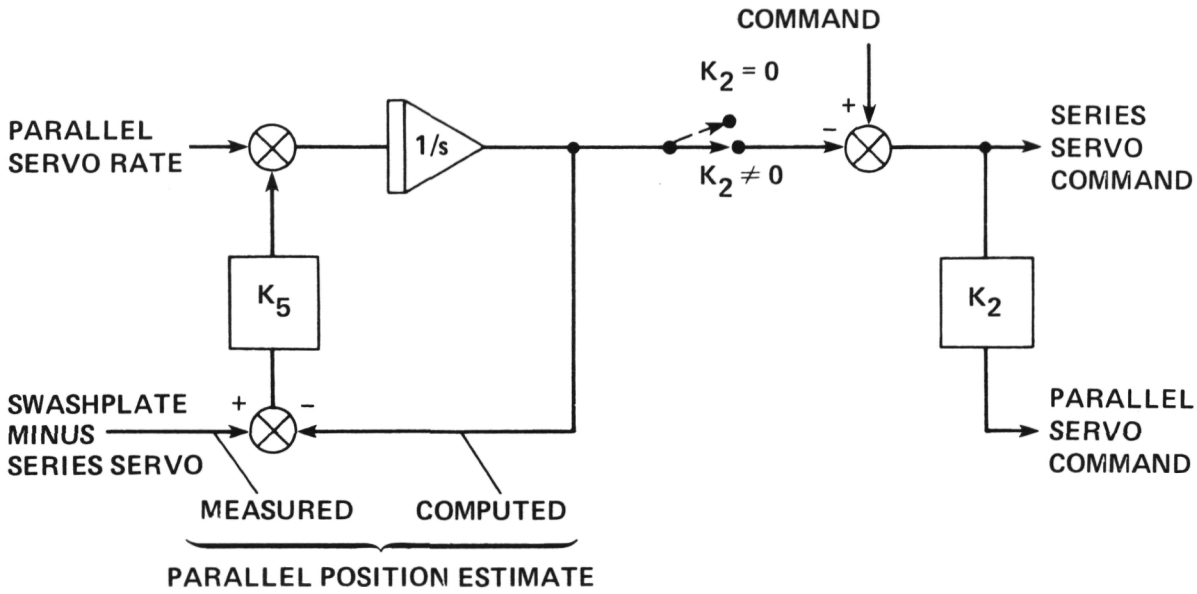

Figure 26.- UH-1H VSTOLAND parallel servo drive.

1. Report No.	2. Government Accession No.	3. Recipient's Catalog No.
NASA TM 84376		

4. Title and Subtitle	5. Report Date
A HELICOPTER FLIGHT INVESTIGATION OF ROLL-CONTROL SENSITIVITY, DAMPING, AND CROSS-COUPLING IN A LOW-ALTITUDE LATERAL MANEUVERING TASK	December 1983
	6. Performing Organization Code
7. Author(s)	8. Performing Organization Report No.
Lloyd D. Corliss and Dean Carico	A-9431
	10. Work Unit No. T-6292
9. Performing Organization Name and Address	11. Contract or Grant No.
Ames Research Center and AVRADCOM Research and Technology Laboratories Moffett Field, Calif. 94035	
	13. Type of Report and Period Covered
12. Sponsoring Agency Name and Address	Technical Memorandum
National Aeronautics and Space Administration, Washington, D.C. 20546 and U.S. Army Aviation Research and Development Command, St. Louis, Mo. 63166	14. Sponsoring Agency Code

15. Supplementary Notes

Point of contact: Lloyd D. Corliss, AVRADCOM Research and Technology Laboratories, Ames Research Center, Moffett Field, CA 94035, (415)965-6269 or FTS 448-6269

16. Abstract

A helicopter in-flight simulation was conducted to determine the effects of variations in roll damping, roll sensitivity, and pitch- and roll-rate cross-coupling on helicopter flying qualities in a low-altitude maneuver. The experiment utilized the Ames UH-1H helicopter in-flight simulator, which is equipped with the V/STOLAND avionics system. The response envelope of this vehicle allowed simulation of configurations with low-to-moderate damping and sensitivity. A visual, low-level slalom course was set up, consisting of constant-speed and constant-altitude S-turns around the 1000-ft markers of an 8000-ft runway. Results are shown in terms of Cooper-Harper pilot ratings, pilot commentary, and statistical and frequency analyses of the lateral characteristics. These results show good consistency with previous ground-simulator results and are compared with existing flying-qualities criteria, such as those set forth in MIL-F-83300 and MIL-H-8501A.

17. Key Words (Suggested by Author(s))	18. Distribution Statement
Helicopter Helicopter handling qualities NOE	Unlimited Subject category - 08

19. Security Classif. (of this report)	20. Security Classif. (of this page)	21. No. of Pages	22. Price*
Unclassified	Unclassified	50	A03

*For sale by the National Technical Information Service, Springfield, Virginia 22161